IJESG

International Journal of Energy and Smart Grid

INESEG

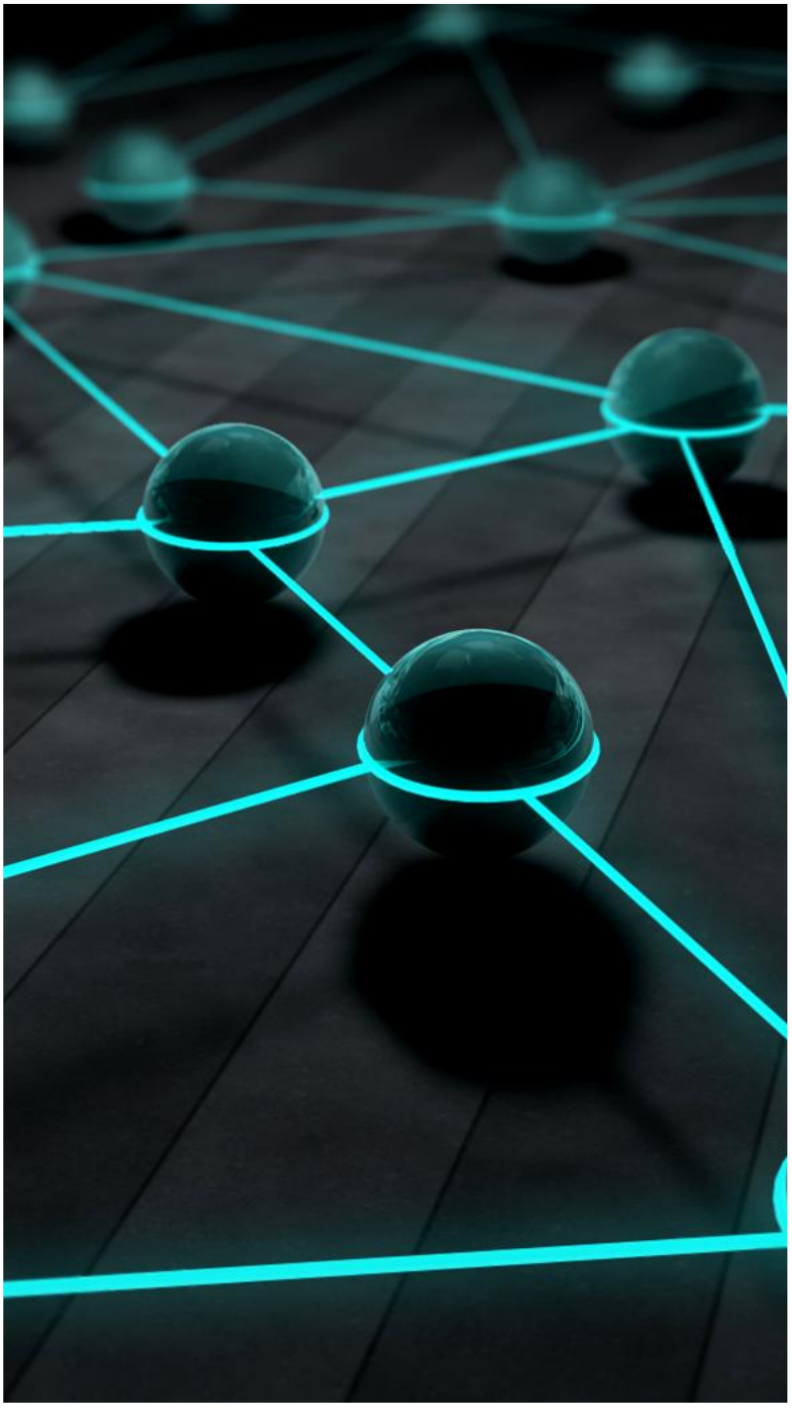

Volume 5
Issue 1-2
2020

ISSN :2548-0332
e-ISSN:2636-7904

Email (for orders and customer services enquiries) : info@ineseg.org, ijesg@ineseg.com
Visit our home page on www.dergipark.org.tr/ijesg

EDITORIAL BOARD MEMBERS

Publisher of Journal: Bilal Gümüş (INESEG)

REVIEWERS IN THIS ISSUE

Dr. Yurdagül Benteşen Yakut
Dr. M.Emin Asker
Dr. Heybet Kılıç
Dr. Hasan Bayındır
Dr. Fatih Koçyiğit
Dr. Orhan Arpa
PhD(c) Cem Haydaroğlu

INESEG

IJESG Vol 5, Number 1-2, 2020
International Journal of Energy and Smart Grid
ISSN: 2548-0332 e-ISSN: 2636-7904

INESEG

CONTENTS

IJESG International Journal of Energy and Smart Grid
Vol 5, Number 1, 2020
ISSN: 2548-0332 e-ISSN 2636-7904

INESEG

A REVIEW OF THE BIODIESEL SOURCES AND PRODUCTION METHODS

Ezgi Sühel AKTAŞ[1], Özlem DEMİR[2*], Deniz UÇAR[2]

[1]Harran Üniversity, Graduate School of Natural and Applied Science, Şanlıurfa/ TURKEY
[2]Harran University, Engineering Faculty, Environmental Engineering Department, Şanlıurfa/TURKEY
[*]Corresponding author: odemir@harran.edu.tr

ABSTRACT

As a result of the rapidly growing population and the developing industry, energy resources are becoming exhausted and therefore it is becoming increasingly necessary to find alternative energy sources. An alternative fuel must be technically feasible, economical, environmentally friendly. One of the alternative fuels is biodiesel. Biodiesel is an alternative, non-toxic, biodegradable and renewable fuel obtained from renewable energy sources. Vegetable oils from oilseed crops such as biodiesel, rapeseed (canola), sunflower, soybean, safflower, animal fats, short chain alcoholic waste in the presence of catalyst can be obtained from home frying oils. Biodiesel does not contain oil; but it can be used as a fuel by mixing it with pure or any oil based diesel. In other words, biodiesel is mono alkyl esters obtained by reaction of vegetable fatty acid esters under certain conditions with simple alcohols such as methanol or ethanol. The types of vegetable oil used as a source of raw materials in biodiesel production are very important. Because the types and ratios of the fatty acids in the oil used indicate the fuel quality of the produced biodiesel. Biodiesel is produced by dilution, microemulsion, pyrolysis and transesterification. In addition, there are studies to treat the wastewater produced during biodiesel production.

In this study, after giving general information about biodiesel and its sources, production methods are discussed in detail. A sample study on the treatment of wastewater generated during the production of biodiesel is also included.

Key Words: Biodiesel, biodiesel production, biomass energy, biodiesel production methods

1.Introduction

1.1.Biodiesel

One of the most important elements of human beings is energy. Petrochemical resources, coal and natural gas make up a large portion of the world's energy needs. As the world's energy needs increase day by day, interest in energy resources has started to increase.

80% of the energy sources used supply of fossil fuels. 70% of fossil fuels are coal, 20% are petroleum and 10% are natural gas [1]. According to the analyses made in line with the utilization rates of the fossil resources, the amount of reservoirs of the existing reserves will decrease substantially in 100 years. Moreover, considering the CO_2 emissions of fossil fuels, environmental pollution is estimated to increase by 50% in the 2030s [2]. In recent years, oil resources have been decreasing and therefore finding alternative energy sources has become an obligation. Among these

methods, renewable biomass Energy is of great importance. Substances of animal and vegetable origin are classified as biomass energy sources [3].

As an alternative fuel, one of the fuels that are being studied is; It is biodiesel. Biodiesel is an alternative diesel fuel obtained from renewable sources. Biodiesel is produced by reacting vegetable or animal oils with an alcohol and catalyst. It is also a non-toxic, biodegradable and renewable diesel fuel.

Fatty acid alkyl ester derived from oil seed plants such as biodiesel, rapeseed, canola, sunflower, soybean, safflower, animal fats, waste domestic frying oils with a short chain alcohol accompanied by a catalyst is a chemical product of alkyl ester. Biodiesel does not contain oil; but can be used as a fuel, either pure or mixed with diesel oil of any proportion [4]. In other words, biodiesel are mono alkyl esters obtained by reacting vegetable fatty acid esters with simple alcohols such as methanol or ethanol under certain conditions [5].

In this study, after giving general information about biodiesel and its sources, production methods are discussed in detail. In addition, in this study, a study on advanced oxidation methods has been extensively included.

2. Biodiesel Resources

Biodiesel, vegetable and animal oils, recovery oils, municipal and industrial waste origin recovery oils, waste vegetable oils, used frying oils and algae are produced.

Oil sources that can be used in biodiesel production:

- **Vegetable Oils:** Sunflower, Soybean, Rapeseed, Safflower, Cotton, Palm Oils
- **Recovery Oils:** Vegetable Oil Industry By-Products
- **Urban and Industrial Waste Origin Recovery Oils**
- **Animal Oils:** Frost Oils, Fish Oils and Poultry Oils
- **Waste Vegetable Oils:** Used Cooking Oils

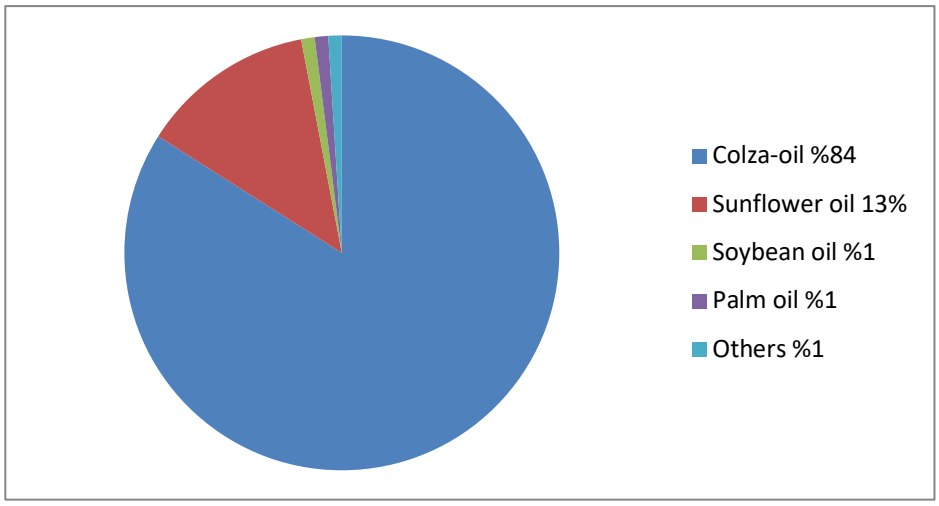

Figure 1. Sources of raw materials used in biodiesel production [6]

Figure 1 shows the distribution of raw material resources used in biodiesel production. Accordingly, rapeseed oil is the most used raw material with 84%, followed by sunflower oil with

13%. Soybean, palm oil and other raw materials have a share of 1% in production. Rapeseed oil (canola oil) is the most important type of vegetable oil used in transesterification and canola oil is very suitable for high quality biodiesel production. Germany and Austria are the leading countries in the production of canola-based biodiesel. Sunflower oil is widely used in biodiesel production in Southern France and Italy, soybean oil in USA, palm oil in Malaysia. The USA, Austria and the UK are the leader countries that produce biodiesel based on used cooking oil. The most important problem in biodiesel production is the regular and continuous supply of raw materials [6].

The type and amount of vegetable oils used as raw material sources in biodiesel production are very important. Because the types and proportions of the fatty acids in the oil used show the fuel quality of the biodiesel produced.

3.Biodiesel Production

3.1.Dilution Process

Dilution process; is a process of thinning vegetable and waste oils by mixing with a solvent or a diesel fuel in certain proportions. The most common of these processes is the mixing of oils with diesel fuel. This reduces oil viscosity and reduces diesel fuel utilization [7]. In the applications, mixing ratios of oils with diesel fuels are expressed as: B20, B30, B40, B50, B80. In short, there are 20%, 30%, 40%, 50% and 80% vegetable, animal or waste oil. Oils used in the dilution method of biodiesel production; peanut oil, rapeseed oil, sunflower oil and waste oils [8].

3.2.Microemulsion Creation Method

Another method used to reduce the high viscosity of vegetable oils is microemulsion with short-chain alcohols such as methanol, ethanol or 1-butanol. Microemulsion is the equilibrium distribution of optically isotropic liquid microstructures with dimensions between 1 and 50 nm, normally formed by a combination of two immiscible liquids and one or more active substances [9].

The short-chain alcohol methyl and ethyl alcohol have the disadvantage that the microemulsified vegetable oil has lower heat values than the petroleum diesel fuel due to the presence of alcohol.

3.3.Pyrolysis Method

Pyrolysis consists of thermal decomposition of oils in the presence of air or nitrogen gas. The fuel obtained by pyrolysis can be made cheaper than that obtained by transesterification. This is possible using low quality raw materials. For example; Pyrolysis can be used as raw material for restaurants' food oil wastes, transesterification process oil wastes and oil products from factories producing food oil [10].

Pyrolysis is firstly decomposed by heat energy in a closed container of vegetable oils. Secondly, the prepared materials are decomposed as thermal energy by distillation and vegetable and waste oils and the obtained biodiesel shows similar properties to diesel fuels.

In this method, vegetable oil molecules are broken down into smaller molecules in an oxygen-free environment at high temperature. This process takes place in the form of separations at C-C or C-H bonds. This process is divided into three parts: hydro cracking, catalytic cracking and thermal cracking. The amount of product produced depends on the method used and the reaction parameters. For example, solid product is obtained at low reaction rates at low temperatures and more liquid product is obtained by cracking operations performed in a short time with rapid temperature increase.

IJESG International Journal of Energy and Smart Grid
Vol 5, Number 1, 2020
ISSN: 2548-0332 e-ISSN 2636-7904
INESEG

In the pyrolysis process, although the fuel properties of vegetable oils approach to diesel fuel properties, high energy consumption is the most important disadvantage [9].

The pyrolysis method is a good method for the evaluation of industrial wastes and urban wastes besides obtaining fuel. Pyrolysis is also an easy and efficient method among other methods [11].

3.4.Transesterification Method

Transesterification is the most common way to produce biodiesel. Transesterification is the general term used to describe the conversion of one ester to another by exchange of alkoxide groups, the class of important organic reactions in which one ester is being converted. Of all alternatives, transesterification is considered the best choice because it is relatively simple for this process [12].

Biodiesel is obtained from vegetable oils by transesterification reaction (alcoholysis). In the transesterification reaction, the oil is esterified with a mono hydric alcohol (ethanol, methanol), giving fatty acid esters and glycerin as the main product in the presence of catalyst (acidic, basic catalysts and enzymes). In addition, in the esterification reaction diglycerides and monoglycerides, excess reactants and free fatty acids are formed. Rapeseed, sunflower, soy and used frying oils, methanol as alcohol, alkali catalysts (sodium or potassium hydroxide) as catalysts are preferred as biodiesel production. Animal oils can also be used in biodiesel production [13].

Figure 2 shows the transesterification reaction. The triglycerides, the main component of the oil, are converted to mono alkyl esters in the transesterification process. Di- and monoglycerides, excess reactants and free fatty acids are formed as by-products in the esterification reaction. Rapeseed, sunflower, soybean and used frying oils, methanol as alcohol, alkali catalysts (sodium or potassium hydroxide) as catalysts are preferred as biomotor production. Animal fats can also be used in the production of biomotorin. Therefore, the refining stage becomes important. Production is very easy. The degree of purity of biodiesel is the most important point in production. Therefore, the refining stage is very important. Biomotor should be produced over 99% pure. In the transesterification reaction, the main product is esterified with oil, ethanol, methanol, acidic, basic catalysts and fatty acid esters and glycerin in the presence of enzymes.

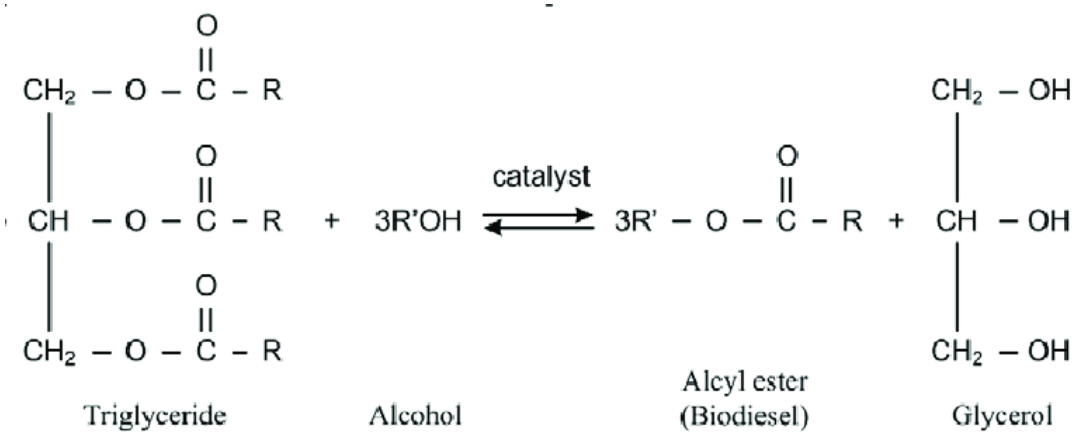

Figure 2: Transesterification Reaction [5]

There is no difficulty in production technology. The most important point in production is the degree of purity of biodiesel. Therefore, the refining stage becomes important. By direct esterification of fatty acids, fatty acids are converted to fatty acid esters with the homogeneous or heterogeneous

catalyst effect of acidic character with alcohol and water is released as well as biodiesel. Since water is more volatile than fatty acid esters, it is possible to achieve very high conversions when removed from the reactor by any method [13].

There are 3 main ways to produce biodiesel from vegetable oils or fats:

- Transesterification with base catalyst
- Acid catalyst transesterification
- Fat is converted to fatty acids and then converted to biodiesel.

The base catalyst transesterification process is most commonly used for biodiesel production. Lower temperature and pressure, minimum side reactions and reaction time and high percentage of conversion (98%), direct conversion to biodiesel without intermediate compounds, no foreign, external substances in the structure are among the reasons [9].

4.Studies Related To Biodiesel

Brito et al., Evaluated the potential of advanced oxidative processes (AOP) in biodiesel wastewater treatment. The efficiency of four AOPs, Fenton, photo-Fenton, solar photo-Fenton and sun-photolysis, was tested by measuring the total organic carbon removal from this residue. Also, the toxicity of the treated residue was investigated by fish embryo tests (FET). Solar photolysis (8 hours exposure to sunlight) has been considered the best treatment, while photo-Fenton, similar to solar photo-Fenton and solar photolysis, leads to reduced organic load. This has been studied in relation to significant organic load reduction (more than 92%) which is easily occurring and a 100% reduction in toxicity for Zebrafish embryos in the dilution range has been studied. In the best cases, about 6-8% of the organic content in biodiesel wastewater is pollutant [14].

Keera et al., investigated the variables affecting the yield and properties of biodiesel produced from vegetable oils The variables studied were reaction time (1-3 hours), catalyst concentration (0.5-1.5% w / w) and oil / methanol molar ratio (1: 3-1: 9). The best yield percentages were obtained using a methanol / oil mole ratio of 6: 1, sodium hydroxide (1%) as catalyst and a temperature of 60 ± 1 ° C for 1 hour. Fatty acid methyl ester (FAME) yield was determined by HPLC and FAME compound by gas chromatography. Biodiesel samples were physicochemically characterized. The results indicate that the biodiesel fuel produced is within the recommended biodiesel fuel standards [15].

Elangoa et al. produced batch-scale biodiesel using castor oil by alkali catalyzed transesterification. Initially, the transesterification parameters such as reaction time, catalyst concentration, reaction temperature and methanol molar ratio in oil: biodiesel production were optimized by the conventional method followed by the statistical-based central composite design method. According to optimized experimental results, 95.9%, 1.25% (w / v) KOH catalyst and a 1:12 oil: methanol mole ratio of 94.9% FAME yield were obtained for 60 minutes reaction. The predicted yield is 93.7%. Purification of crude biodiesel was carried out by simple evaporation and silica gel adsorption. Analytical results showed that significant amounts of methyl ester groups, such as ricinoleic, linolenic, palmitic acid and oleic acid, were present in the biodiesel [16].

The use of ultrasound in biodiesel transesterization Ho et al. Reviewed the developments obtained from different raw materials by using acid, base and enzyme catalysts for ultrasound assisted biodiesel transesterization. For each of these, a critical assessment of the state of the art technology

has focused on the use of ultrasound energy with heterogeneous catalysts. For each of the technologies studied, the reaction parameters and interactions between process efficiency and productivity are discussed and analyzed [17].

Wu et al. developed a new reaction system for the production of biodiesel by base catalyzed transesterization. Bentonite is used as an adsorbent in a conventional homogeneous base catalyzed transester reaction reaction system to form a heterogeneous system that increases reaction homogeneity. By studying the effect of bentonite on NaOH catalyzed methanolysis of soybean oil and the associated reaction mechanisms, it was found that a suitable bentonite input could support methanolysis. By the rapid removal of water from the system, bentonite enhances the conversion of NaOH to catalytically active methoxide species and the major side reactions can be significantly inhibited. The methanolysis of the triglycerides took place in the liquid phase rather than in the solid phase. The introduction of bentonite also reduced the soap concentration in crude biodiesel; this was useful for producing resinous biodiesel after treatment [18].

Navas et al. emphasize the support of CaO, MgO and ZnO on both mass and C-Al_2O_3, as well as the catalytic activity and characterization of transesterification of soybean oil and castor oil with methanol and butanol. XRD, SEM, CO_2 adsorption followed by TGA and N_2 adsorption were used to characterize the prepared catalysts. The presence of C-Al_2O_3 in the supported catalysts improves alcohol degradation in the superficial basic regions. The first step of the reaction mechanism is then preferred (hydrogen abstraction). In transesterification of butanol with castor oil, MgO / C-Al_2O_3 and ZnO / C-Al_2O_3 catalysts showed high yields to FABE (97% and 85%, respectively). These latter catalysts provide an effective alternative to obtain second generation biodiesel, considering that castor oil cannot be a source and butanol is an alcohol obtainable from biomass [19].

Tiwari et al. studied waste oil transesterification using alkali (NaOH) as catalyst, yielding 85% ester (biodiesel) conversion [20].

In the biodiesel pilot plant, Hüseyin et al. used corn oil, chicken oil and animal oil as vegetable oil to produce methyl ester. When the FFA level of corn oil is below 1%, animal oils are too high to produce biodiesel through the base catalyst. For this reason, since pretreatment reaction was required for animal fats, sulfuric acid was used as catalyst and methanol was used as alcohol in pretreatment reactions. After lowering the FFA level of animal fats to less than 1%, the transesterification reaction was completed with alkaline catalyst. Due to the low FFA content of corn oil, it was subjected to direct transesterification. Potassium hydroxide was used as catalyst and methanol was used as alcohol for transesterization reactions. The fuel properties of the methyl esters produced at the biodiesel pilot plant were characterized and compared with EN 14214 and ASTM D6751 biodiesel standards. According to the results, the ester yield values of animal fat methyl esters are slightly lower than corn oil methyl ester (COME). The production cost of COME is higher than the cost of animal fat methyl esters because it is a high cost biodiesel raw material. Produced methyl esters have similar fuel properties. In particular, the sulfur content and cold flow properties of COME are lower than those of animal fat methyl esters. The measured fuel properties of all produced methyl esters met ASTM D6751 (S500) biodiesel fuel standards [21].

İbrahim et al. investigated the experimental optimization of ultrasound-assisted biodiesel production in the presence of heterogeneous catalyst. Three catalysts; For comparison, CaO, calcined

dolomite and calcium diglyceroxide (CaDG) were considered. The D-optimal test plan was subsequently applied to obtain the regression models used to determine the optimum process conditions. The maximum biodiesel yield was calculated as 98.7%, 95.9% and 86.3% for CaO, calcined dolomite and CaDG, respectively. Finally, in the case of CaO catalyst, catalyst loading: 5.35% (oil by weight), methanol / oil ratio: 7.48, ultrasonic power: 40 W, time: 150 min and reaction temperature: 60 ° C yielded maximum biodiesel yield (99.4%) It was [22].

Pali et al. Explorated and developed an indigenous fuel from abundant forest of India. Single stage base catalyst transesterification was employed for biodiesel production. Sal seeds was used biodiesel production in India due to its low acid value. Cetane number, viscosity, calorific value and cold filter plugging point (CFPP) were optimized using response surface methodology (RSM). Methanol to oil molar ratio (3–15:1), KOH catalyst concentration (2.5–15 g/kg), reaction time (30–120 min) and reaction temperature (50–70 °C) were optimized. Results were validated through the confirmation trails and all properties of Sal biodiesel are well within ASTM limits. The results showed that Sal seed is the needed source of biodiesel in India [23].

Zahan and Kano's article discusses the properties of biodiesel, the difference between palm-biodiesel and other biodiesel sources, and the feasibility of using palm oil as a primary source for future alternative and sustainable energy sources. According to the results of the study, it is predicted that the future trends of Palm-biodiesel will likely move towards the balance between the community and market demands and consumer perceptions. With this study, palm oil by-products and mill waste were proposed as future raw materials for biodiesel due to their cheaper costs, availability, abundance, environmental friendliness and minimal effects on food safety. New research is needed to improve product quality and particularly to solve other environmental issues [24].

In the study by Raoufi and Gargari, the optimized lipase A (Lip A) gene from Pseudomonas aeruginosa was fused with GPI's protein Gcw61 and is on the surface of Pichia pastoris X33. Copy numbers of the added lipase gene, actual values are used as 2.09 ± 0.06 by PCR absolute quantification method. Some detergents appear to significantly reduce enzyme activity. The results show that all cell biocatalysts show good potential for the production of biodiesel from microalgae oil in 10 repeat batch cycles [25]

5.Advanced Oxidation Methods And A Case Fenton Process Study From Literature For The Treatment Of Biodiesel Wastewater

In a case study from the lietaruture related to the Fenton Process in order to treat biodisel wastewater four different processes were applied: biodiesel wastewater, Fenton, photo-Fenton, solar photo-Fenton and solar photolysis. The aim is to compare the efficiency of the selected treatment processes and to provide safe alternatives for the disposal of biodiesel wastewater. Fenton and photo-Fenton were performed in triplicate in three sets of glass reactors held under constant magnetic stirring by temperature monitoring. Solar experiments (outdoor) were performed twice and each reactor set was homogenized when [H_2O_2] was added (every 15 minutes). For solar experiments, radiation was monitored using a radiometer (Sunlight, PMA 2120). Prior to TOC analysis, all samples were filled to their original volumes by addition of deionized water (typically 5-10 mL) [14].

5.1.Fenton Reactions

Based on the studies of Grčić et al., 180-minute pre-tests (2014) and Sabaikai et al. (2014) using Fe $^{2+}$ ranging from 20 to 50 mg of L-1 and H_2O_2 to 100 to 1000 mg/L. The best results were obtained using [Fe^{2+}] = 20 mg/L and [H_2O_2] = 1000 mg/L. Based on these results, [Fe^{2+}] = 20 mg/L and [H_2O_2] = 1000 mg/L were used in all other experiments. Experiments using the Fenton reaction were performed in closed glass containers wrapped in aluminum foil. A 100 mL sample was taken from the biodiesel waste water and $FeSO_4.7H_2O$ (FMAIA P.A.) was then added to obtain an iron ion concentration of 20 mg/L. H_2O_2 (Vetec 30%) was added to give a constant concentration of 1000 mg/L every 1000 minutes. The procedure lasted 300 minutes with TOC monitored every 30 minutes [14].

5.2.Photo-Fenton Reaction

This reaction was carried out in 100 mL of biodiesel waste water using the same concentration of iron ions (20 mg L-1) used for the Fenton reaction. Hydrogen peroxide was added every 15 minutes to give a constant concentration of 1000 mg/L. The sample was also irradiated with UV light provided by a high pressure mercury vapor lamp (125 W) (λ = 254 nm). This process lasted 480 minutes and the TOC was measured every 30 minutes [14].

5.3. Solar Photo-Fenton

Experiments were performed using the same conditions as the photo-Fenton reaction (point 2.2.4) but using solar radiation instead of mercury lamp. A 500 mL biodiesel wastewater sample was placed in a glass receiver (29.6 cm x 17.8 cm x 5 cm) and exposed. After the addition of Fe^{2+} (20 mg/L), 1.25 mL of H_2O_2 (1000 mg/L) was added periodically to natural sunlight (outdoor) and every 60 minutes. The experiment lasted 480 minutes (in May 2016 in Midwestern Brazil). TOC content was measured every 60 minutes [14].

5.4.Solar Photolysis

These experiments were performed in a similar way to solar photo-Fenton. It consisted of exposing 500 mL of biodiesel wastewater (in a 29.6 cm x 17.8 cm x 5 cm glass receiver) to sunlight for 480 minutes (in May 2016, Central Brazil). The TOC content was measured every 60 minutes. The solar experiments were continued for the next 180 minutes. This step aimed to assess whether the treatment was at its end [14].

6.Conclusion

As a result of literature studies; Although fossil fuels cause environmental pollution in recent years, they are decreasing rapidly as they are alternative energy sources. Therefore, studies have been started on alternative fuels and it has been determined that biodiesel obtained from vegetable and animal oils can be used as an alternative fuel that can be produced from renewable sources. Biodiesel is a non-toxic, biodegradable and renewable diesel fuel that can be easily dissolved in soil without damaging the environment. Transesterification, a chemical process that converts vegetable oils into an alternative fuel, reduces viscosity. It contains high cetane number, renewable property, high combustion efficiency and low emulsion. Studies on the treatment of wastewater generated during the

production of biodiesel are not common, but it is possible to come across in the literature. Fenton, which uses advanced oxidation processes for the treatment of this wastewater, has also been demonstrated. However, further studies are needed to establish effective methods for wastewater treatment.

References

[1] N. L. Panwar, S. C. Kaushik, and S. Kothari, "Role of renewable energy sources in environmental protection : A review," *Renew. Sustain. Energy Rev.*, vol. 15, no. 3, pp. 1513–1524, 2011.

[2] E. K. Stigka, J. A. Paravantis, and G. K. Mihalakakou, "Social acceptance of renewable energy sources : A review of contingent valuation applications," *Renew. Sustain. Energy Rev.*, vol. 32, pp. 100–106, 2014.

[3] I. Kralova and J. Sjöblom, "Biofuels-renewable energy sources: A review," *J. Dispers. Sci. Technol.*, vol. 31, no. 3, pp. 409–425, 2010.

[4] H. Ölmez, "Alternatif Bir Enerji Kaynağı," Ondokuz Mayıs Üniversitesi, 2005.

[5] A. S. Altınsoy, "Biyodizel Üretimi, Motorlarda Kullanımı ve Türkiye'deki Kaynakların İncelenmesi," İstanbul Teknik Üniversity, Graduate School of Natural and Applied Sciences, Master Thesis, 2007.

[6] R. Demirbilek, "Biodizel," Yıldız Tecnical Üniversity, Reseach Project, 2008.

[7] N. Tippayawong, P. Chumjai, and A. S. Preparation, "Characterization and Performance of Biofuel from Passion Fruit Processing Residues," *Proc. World Congr. Eng. Comput. Sci. 2012 Vol II WCECS 2012, Oct. 24-26, 2012, San Fr. USA*, vol. II, pp. 24–27, 2012.

[8] T. Eryılmaz, "Yozgat İli Şartlarında Yetiştirilen Aspir (Carthamus tinctorius L.) Dinçer Çeşidinden Üretilen Biyodizelin Yakıt Özelliklerinin Belirlenmesi," Journal of *Gaziosmanpaşa University.* Agricultural Faculty, 2014.

[9] İ. Yüce, "Alternatif Yakıt Olarak Biyodizelin Türkiye'deki Ve Almanya'daki Durumu İle Taşıtlarda Kullanımının İncelenmesi," İstanbul Technical University, Mechanical Engineering, Master Thesis, 2008.

[10] C. Zhenyi, J. I. Xing, L. I. Shuyuan, and L. I. Li, "Thermodynamics Calculation of the Pyrolysis of Vegetable Oils Thermodynamics Calculation of the Pyrolysis," *Energy Sources Energy Sources, 269, 849-856, DOI 10.1080/00908310490465902*, vol. 8312, 2004.

[11] A. Kaya, "Kızartma Atığı Yağlarından Süperkritik Alkol Transesterifikasyon Yöntemi İle Biyodizel Elde Edilmesi," Selçuk University, Graduate School of Natural and Applied Sciences, Chemical Engineering, Master Thesis, 2007.

[12] M. G. Gomes, D. Q. Santos, L. C. De Morais, and D. Pasquini, "Purification of biodiesel by dry washing, employing starch and cellulose as natural adsorbents," *Fuel*, vol. 155, pp. 1–6, 2015.

[13] M. M. Nayır, "Kanola Yağından Baz Katalizli Transesterifikasyon Yöntemi İle Biyodizel Üretiminde Reaksiyon Parametrelerinin Optimizasyonu," Ondokuz Mayıs University, Chemical Engineering, Master Thesis, 2018.

[14] S. Brito, "Evaluation of advanced oxidative processes in biodiesel wastewater treatment," *J. Photochem. Photobiol. A Chem.*, vol. 375, pp. 85–90, 2019.

[15] S. T. Keera, S. M. El Sabagh, and A. R. Taman, "Transesterification of vegetable oil to biodiesel fuel using alkaline catalyst," *Elsevier*, vol. 90, no. 1, pp. 42–47, 2011.

[16] R. K. Elango, K. Sathiasivan, C. Muthukumaran, V. Thangavelu, M. Rajesh, and K. Tamilarasan, "Transesterification of castor oil for biodiesel production: Process optimization and characterization," *Appl. Therm. Eng.*, vol. 145, pp. 1162–1168, 2019.

[17] W. W. S. Ho, H. K. Ng, and S. Gan, "Advances in ultrasound-assisted transesterification for biodiesel production," *Appl. Therm. Eng.*, vol. 100, pp. 553–563, 2016.

[18] L. Wu, T. Wei, Z. Tong, Y. Zou, Z. Lin, and J. Sun, "Bentonite-enhanced biodiesel production by NaOH-catalyzed transesteri fi cation of soybean oil with methanol ☆," *Fuel Process. Technol.*, vol. 144, pp. 334–340, 2016.

[19] M. B. Navas, I. D. Lick, P. A. Bolla, M. L. Casella, and J. F. Ruggera, "Transesterification of soybean and castor oil with methanol and butanol using heterogeneous basic catalysts to obtain biodiesel," *Chem. Eng. Sci.*, vol. 187, pp. 444–454, 2018.

[20] S. Tiwari, "Optimization of transesterification process for biodiesel production from waste oil," *Int. J. Pharm. Life Sci.*, vol. 4, no. 6, pp. 2701–2704, 2013.

[21] E. Alptekin, M. Canakci, and H. Sanli, "Biodiesel production from vegetable oil and waste animal fats in a pilot plant," *Waste Manag.*, vol. 34, no. 11, pp. 2146–2154, 2014.

[22] I. Korkut and M. Bayramoglu, "Selection of catalyst and reaction conditions for ultrasound assisted biodiesel production from canola oil," *Renew. Energy*, vol. 116, pp. 543–551, 2018.

[23] H. S. Pali, A. Sharma, Y. Singh, N. Kumar, " Sal biodiesel production using Indian abundant forest feedstock," *Fuel, vol.275,* 117781, 2020.

[24] K. A. Zahan and M. Kano, "Biodiesel Production from Palm Oil, Its By-Products, and Mill Effluent: A Review,"Energies*,11*, 2132, 2018.

[25] Z. Raoufi and S. L.M. Gargari, " Biodiesel production from microalgae oil by lipase from *Pseudomonas aeruginosa* displayed on yeast cell surface, *Biochemical Engineering Journal,*Volume 140, pp.1-8, 2018

IJESG International Journal of Energy and Smart Grid
Vol 5, Number 1-2, 2020
ISSN: 2548-0332 e-ISSN 2636-7904

INESEG

DESIGN, CONSTRUCTION AND PERFORMANCE ASSESSMENT OF A HYBRID SOLAR DRYER USING FORCED CONVECTION PRINCIPLE

Jamilu Ya'u MUHAMMAD [1*], Adamu Yusuf ABDULLAHI[2], Ibrahim Bako ABDULHAMID[3], Auwal Bala ABDULKADIR[1], Ibrahim Umar IBRAHIM[4], Mahmoud Mukhtar MAIKUDI[5], Mustapha Alhassan ALIYU[6]

[*1]Department of Mechanical Engineering, Bayero University, Kano, Nigeria

[2]Department of Mechatronic Engineering, Bayero University, Kano, Nigeria

[3]Department of Pure and Applied Physics, Federal University Wukari, Taraba, Nigeria

[4]National Space Research and Development Agency, Nigeria

[5]Nigeria Defense Academy, Kaduna, Nigeria

[6]Department of Physics, Bayero University, Kano, Nigeria

[*] Corresponding author; E-mail: muhdjy87@gmail.com

Abstract

In developing countries like Nigeria, local farmers are always facing challenges on drying and preservation of the agricultural products after harvesting due to losses in quality and quantity of the products by using local drying method, to address the problem, solar drying system is used. This study presented design, construction and performance assessment of a hybrid solar dryer using forced convection principle for drying of tomato slices. The system consists of solar collector, drying chamber with four drying trays, solar photovoltaic for powering fans and adding more heating in the evening and/or cloudy hours and chimney. The result revealed that for all the testing days, the air temperatures at the drying chamber were greater than that at ambient, solar collector and chimney outlet. It was also found that the solar dryer has a drying rate of 0.274kg/hr while the dryer efficiency and collector's efficiency were 50.2% and 43.03% respectively. It was recommended that the solar drying system should be used to dry and preserve the agricultural products without losses in quality and quantity of the products.

Key words: *Air Temperature, Chimney, Drying Chamber, Relative Humidity, Solar Collector*

IJESG International Journal of Energy and Smart Grid
Vol 4, Number 1, 2019
ISSN: 2548-0332 e-ISSN 2636-7904
doi: 10.23884/IJESG.

1. Introduction

Nowadays, in order to maintain the quality of most agricultural products (Cereals, Fruits, Vegetables) after harvesting, they need to be dried and preserved. Therefore, drying has become very important in the agricultural sector.

It was found that when the temperature of the agricultural products (Cereals, Fruits and Vegetables) reaches 271°K, the contaminated micro-organism were killed away from the products, this will prevent about 10% and 20% bacteria, yeast, moulds and enzymes of agricultural products from spoiling by reducing the moisture content of the products [1]. Traditionally, farmers used some food preservation techniques such as drying, refrigeration, freezing, salting (curing), sugaring, smoking, pickling, canning and bottling. The traditional drying is known as direct (open) sun drying and it is common and widely used method for drying agricultural products, although it is simplest and cheapest method but it includes contaminations, losses, damage by birds or insects and slow drying [2-5]. Lack of foodstuffs in developing countries like Nigeria is links to this local drying method that cause significant losses with is estimated as 40% [6, 7].

Solar thermal technology as one of the wider applicable solar energy technologies, it is also playing vital role in agricultural application due to it nature of abundantly, non-polluting and inexhaustible [8-11]. In tropic areas, where there is at least six (6) hours of sunshine, solar dryer is higher important for the farmers to dry the moisture contents of the agricultural products [12]. Solar drying has many advantages such as time saving, free, low cost of maintenance, improvement of the product quality, environmental protection, and control of required air condition [13-20].

Solar dryer is basically divided into two types namely passive (Natural Convection) solar dryer and active (Forced Convection) solar dryer. Passive solar dryer is also sub-divided into direct, indirect and mixed-mode passive solar dryer while active solar dryer is divided into direct, indirect and hybrid active solar dryer [21, 22].

In indirect dryers, solar energy collected by the solar collector is passing to the drying chamber where the drying products are sprayed on the trays, and the mixed-mode type of dryer has the same operations with the indirect solar dryer but the different is that the wall or roofing of the dryer are made up of transparent materials with high absorbance of solar energy. Whereas direct solar dryers, the drying products are arranged on the plate tray inside the solar collector with the transparent cover through which the solar energy is passed by radiation and the heat is absorbed by the drying products by means of conduction [23].

Hot air is circulating to the drying chamber using fans in forced convection dryers, while in natural convection dryer fan is not used to circulate the hot air. Forced convection dryer is more efficient than the natural convection dryer since the hot air is circulating to the drying chamber, this will yield high rate of drying of the agricultural products [15, 24].

One of the limitations of forced convection dryer, it may not be applicable in rural areas since it required fan and a source of electricity is required to drive the fan [25]. Hybrid solar dryer is a dryer that has a combination of two or more energy sources. It makes use of solar energy during the day and an

IJESG International Journal of Energy and Smart Grid
Vol 4, Number 1, 2019
ISSN: 2548-0332 e-ISSN 2636-7904
doi: 10.23884/IJESG.

alternate energy source at night. The alternate source of energy could be electricity, diesel, biomass or solar PV which is used to powered the fan in forced convection solar dryer [26].

2. Materials and Method

2.1. System's Description

The hybrid dryer consists of four components namely; solar collector, drying chamber, solar photovoltaic and chimney. The solar collector is used to absorb solar radiation and convert it to heat energy, this energy is then passed to the drying chamber where the drying products are arranged on the trays of the drying chamber. The solar collector used in this study is double passed air collector in order to increase the amount of air entering to the solar collector opened at one end to allow atmospheric air enters into it while another end was connected to the drying chamber. The solar dryer is using forced convection principle; therefore, the fan was placed at the air inlet of the drying chamber, this fan pushes the air into the drying chamber in the morning and it used to circulate the inside air at night.

The drying chamber contains four (4) trays which is made up of wire mesh on which the agricultural products spread on. The chimney was provided on top of the drying chamber to decrease the relative humidity of the air around the drying chamber, facilitate and control the convective flow of air through the drying chamber and the chimney has cover to prevent water or rain from entering the drying chamber. The two opposite sides of the drying chamber were glazed to collect additional solar radiation. A side door was provided for ease access with trays when loading and offloading of the drying products. The thermal storage material was sprayed on the bottom of the drying chamber which heat the air in the drying chamber, and it will reduce its moisture content because the storage material has adsorptive characteristic. The solar photovoltaic was used to generate electricity which will then be used to power the fan.

2.2. Materials Selection

Materials used for construction of the system was selected based on cost, reliability, functionality and processability of the materials.

Table 1 shows the components of the system, materials used and reason(s) for selections:

IJESG International Journal of Energy and Smart Grid
Vol 4, Number 1, 2019
ISSN: 2548-0332 e-ISSN 2636-7904
doi: 10.23884/IJESG.

Table 1: Materials Selected for Construction of the System

Components		Materials Selected	Reason(s)
Solar Collector	Absorber Plate	Galvanized Iron Sheet	High solar radiation absorption, thermal emissivity, corrosion resistance and strong [27]
	Glazing	Perspex glass	Cheap, ease to processing and strong [28]
	Insulation	Sawdust	Cheap and availability
	Frame Cover	Plywood	Cheap, ease to process and strong [28]
	Black Pebbles	Rocks	Cheap, ease to process and strong [28]
Drying Chamber`	Chamber Cover	Plywood/Silica Glass	Availability, reliability and ease processing [28]
	Tray	Wire mesh	Maintainability, strong and cheap
	Chimney	Mild steel	Low cost and ease processing [27]
	Thermal Storage material	Gravels	High insolation and absorption characteristics
Solar Photovoltaic		Polycrystalline Silicon	High solar radiation absorption
Supporting Stand		Mild steel	Cheap, ease to process and strong [28]

2.3. Design Considerations and Assumptions

The following were considered or/and assumed in designing of forced convection hybrid solar dryer:

i. The effect of dust on the solar collector and solar photovoltaic are negligible.
ii. The solar collector operates under steady state conditions.
iii. The amount of solar irradiance falling on the collector and photovoltaic to be available.
iv. The amount of moisture from the fresh agricultural products to be removed.

2.4. System's Components Desisgn

The components of the solar dryer were designed based on the materials selected as follows:

IJESG International Journal of Energy and Smart Grid
Vol 4, Number 1, 2019
ISSN: 2548-0332 e-ISSN 2636-7904
doi: 10.23884/IJESG.

2.4.1 *Design of the Solar Collector*

a. Energy Balance for Solar Collector

For the solar collector to be properly designed, the heat gained by the collector must be equal to the heat lost by the collector [8].

$$Heat\ Energy\ Gained = Heat\ Energy\ Lost$$

$$I_T A_c = Q_u + Q_l + Q_p \quad (1)$$

But $Q_u = \alpha\tau I_T A_c - Q_l$, $Q_l = Q_{Cond} + Q_{Conv} + Q_R$ and $Q_p = \rho\tau I_T A_c$

Where:

I_T = total amount of solar irradiance harnessed by the absorber's surface (Wm^{-2});

A_c = area of the collector (m^2);

Q_u = rate of useful energy collected by the air (W);

Q_{cond} = amount of conduction losses from the absorber (W);

Q_{conv} = amount of convective losses from the absorber (W);

Q_R = amount of long wave re-radiation from the absorber (W);

Q_ρ = amount of reflection losses from the absorber (W);

τ = transmittance of the top glazing(dimensionless);

ρ= coefficient of reflection of the absorber and

α = solar absorptance (dimensionless)

If τ is the transmittance of the top glazing and I_T is the total solar radiation incident on the top surface, therefore, $I_T A_c = \tau I_T A_c$ and $Q_l = U_l A_c (T_c - T_a)$

Where: U_L = overall heat transfer coefficient of the absorber ($Wm^{-2}K^{-1}$); T_c = temperature of the collector's absorber (K) and T_a = ambient air temperature (K).

Therefore, the useful energy gained by the collector is expressed as:

$$Q_u = \alpha\tau I_T A_c - U_l A_c (T_c - T_a) \quad (2)$$

Finally, the energy absorbed per unit area (q_u) by the collector will become:

$$q_u = \alpha\tau I_T - U_l (T_c - T_a) \quad (3)$$

The heat gained by air (Q_g) is given as [29]:

$$Q_g = \dot{m}_a C_{pa} (T_c - T_a) \quad (4)$$

Where $\dot{m}_a$ is mass flow rate of air through the dryer per unit time (kg/s) and C_{pa} is the specific heat capacity of air (kJ/kg K).

The heat removal factor (F_R) in the collector can be calculated using expression given by [30]:

$$F_R = \frac{Q_g}{Q_u} = \frac{\dot{m}_a C_{pa} (T_c - T_a)}{\alpha\tau I_T A_c - U_l A_c (T_c - T_a)} \quad (5)$$

IJESG International Journal of Energy and Smart Grid
Vol 4, Number 1, 2019
ISSN: 2548-0332 e-ISSN 2636-7904
doi: 10.23884/IJESG.

b. Sizing of Solar Collector

Sizing of solar collector is based on meteorological and crop parameters. The required area of the collector for solar dryer is given by [31].

$$A_c = \frac{Q_{load}}{\eta I_T t_d} \quad (6)$$

Where:

Q_{load} is the drying head load (W);

t_d is a drying time (hours) and

η is an efficiency of the collector (%).

The area of the absorber A_{ab} is approximately equal to the area of the collector, A_c; this is related to the length, L_c and width, W of the solar collector as follows:

$$A_{ab} = A_c = L_c \times W \quad (7)$$

2.4.2 Design of Drying Chamber

A. Amount of Moisture to be Removed

The total amount of moisture to be removed (Mw) from the agricultural product is given by [5] as:

$$M_w = W_w \left(\frac{M_i - M_f}{1 - M_f}\right) \quad (8)$$

Where

M_w = amount of moisture removed

W_w = total weight of the products before drying;

M_i = initial moisture content on wet basis and

M_f = final moisture content on wet basis;

B. Energy Balance for Drying Chamber

The amount of heat energy (Q_m) needed to remove moisture from the agricultural product was obtained through the relation [32]:

$$Q_m = M_p C_p \Delta T + M_w L \quad (9)$$

Where:

M_p is the mass of the product to be dried (kg);

Mw is the mass of water removed (kg),

ΔT is the change in temperature in °C and

L is the latent heat of vaporisation of water.

The quantity of heat stored (Q_{hs}) by the heat storage media can be obtained by using the equation [33]:

$$Q_{hs} = M_{hs} C_{hs} \Delta T \quad (10)$$

Where:

M_{hs} is the mass of heat storage medium (kg); and

C_{hs} is the specific heat of the heat storage medium ($kJkgK^{-1}$).

IJESG International Journal of Energy and Smart Grid
Vol 4, Number 1, 2019
ISSN: 2548-0332 e-ISSN 2636-7904
doi: 10.23884/IJESG.

C. Sizing of Drying Chamber

The breadth of the drying chamber, B, is usually equal to the width (W) of the solar collector. Thus, the length of the drying chamber, L_{dc}, is determined from the relation:

$$L_{dc} = \frac{A_{dc}}{W} \quad (11)$$

Where: A_{dc} is the area of drying chamber

2.5. Construction of System's Components and Assembly of the Solar Dryer

The system's components were constructed using the selected materials and available tools. The Tools used in the construction are hammer, handsaw, paint brush, chisel, measuring tape, screw driver, square/straight edges, rolling machine, grinding machine.

2.5.1 Solar Collector

The solar collector sized (1100 x 600 mm) was constructed. The solar collector consists of transparent cover, absorber plate and insulation. Galvanized iron sheet of 2 mm thickness was used for absorber plates and the absorber plates were painted black to increase its solar radiation absorption, the transparent cover is made from 4 mm thickness of Perspex glass. The collector frame was made from plywood and covered it is one end with galvanized wire mesh and a sliding door was attached to control the air flow into the dryer. At outlet of solar collector, a fan was mounted provide the forced convection to the drying chamber. To minimize heat loss from the absorber plate, black pebbles (Rocks) were spreads below the first absorber plate.

2.5.2 Drying Chamber

The drying chamber consist of four (4) trays made up from galvanized wire mesh which is riveted on the wooden frame, to regulate the temperature of the chamber, four (4) thermostats were installed under each tray. The trays are designed to be removable for easier cleaning and loading potential. The two opposite sides of the drying chamber were made from silica glass to increase the amount solar irradiance absorbed. This further increases the convective air flow and additional heating necessary for drying. Access door to the drying chamber was constructed using plywood which is painted black to enhance elevated temperature within the chamber.

A mild steel of 2 mm thickness painted black was used to form a chimney to control the flow of air through the drying chamber. A metallic cup was provided at the top of the chimney to prevent rain, insect and wind from entering the drying chamber. Gravels were spreads at the bottom of the drying chamber as a thermal storage material to absorb heat during the day hours and subsequently dissipate heat at night or during cloud cover.

IJESG International Journal of Energy and Smart Grid
Vol 4, Number 1, 2019
ISSN: 2548-0332 e-ISSN 2636-7904
doi: 10.23884/IJESG.

2.5.3 Solar PV system

The solar photovoltaic module made from polycrystalline silicon rated 200 W was placed on the roof of the drying chamber, a charge controller, an inverter and 150A battery to provide the power for the fan.

The solar collector was oriented facing south and both the solar collector and the roof of the drying chamber tilted at 22.2° to the horizontal. This is 10° more than the local geographical latitude of Kano a location in Nigeria, (12.2° N) [34].

3. Performance Evaluation of Hybrid Solar Dryer

3.1. Experimental Set-up

The hybrid solar dryer was tested to evaluate the performance of the system, the tests were done March, 2020. The tests were conducted for four (4) days, the first day test was done under offload condition (without tomato slices loaded) and the subsequent days under load condition (with tomato slices loaded) starting by 9:00 am with intervals of one (1) hour. The measurement variables included air temperature (ambient, collector, drying chamber and chimney outlet), relative humidity (ambient, drying chamber and chimney outlet), solar radiation intensity, mass of drying tomato slices and wind speed drying air.

After taking reading of the measuring variables under offload condition, the tomato slices were arranged on the dryer tray and the door was closed then the measuring variables were read and recorded with one (1) hour interval starting by 9:00 am for each testing days.

In the evening and/or during cloud days, the door, cover of chimney and sliding door of the inlet of the solar collector were closed in order to maintain the heating condition of the drying chamber, in this case the storage material is giving out the heat storage and used to dry the products.

The temperatures of the hot air were measured using thermocouple device and wire while psychrometer was used to measure the relative humidity of the variables. The anemometer was used to measure the wind speed and amount solar irradiance harnessed by the collector using solarimeter.

3.2. Drying Rate

For the solar dryer to work efficiently, the rate at which the drying products are drying should be known. The drying rate is given by [35] as:

$$R_d = \frac{M_w}{t_d} \tag{12}$$

Where:

R_d is the drying rate (kg/hr), and

M_w is the mass of evaporated water (kg)

3.3. Percentage of Moisture Loss

The percentage of moisture removed from the agricultural products (on wet and dry basis) can be expressed as given by [36] as:

IJESG International Journal of Energy and Smart Grid
Vol 4, Number 1, 2019
ISSN: 2548-0332 e-ISSN 2636-7904
doi: 10.23884/IJESG.

$$MC = \frac{M_1 - M_2}{M_1} \times 100\% \; wet \; basis \quad (13)$$

Where:

MC is the percentage of moisture loss (% wb) and

M_1 and M_2 are the initial and final masses of the drying products respectively (kg).

3.4. Dryer Efficiency

The efficiency of the solar dryer can be found using the relation given by [37] as expressed:

$$\eta_{dryer} = \frac{M_w L}{A_c I_T t_d} \quad (14)$$

3.5. Solar Collector Efficiency

The solar collector efficiency used for solar drying system is related in the expression given by [38] as:

$$\eta_c = \frac{\rho_a v_a c_p \Delta T}{I_T A_c} \quad (15)$$

Where:

V_a is the volumetric flow rate of air (m^3/s), and ρ_a is the density of air.

4. Results and Discussion

Amount of solar irradiance incident on the solar collector for four (4) days of conducting experiments were shown in figure 1.

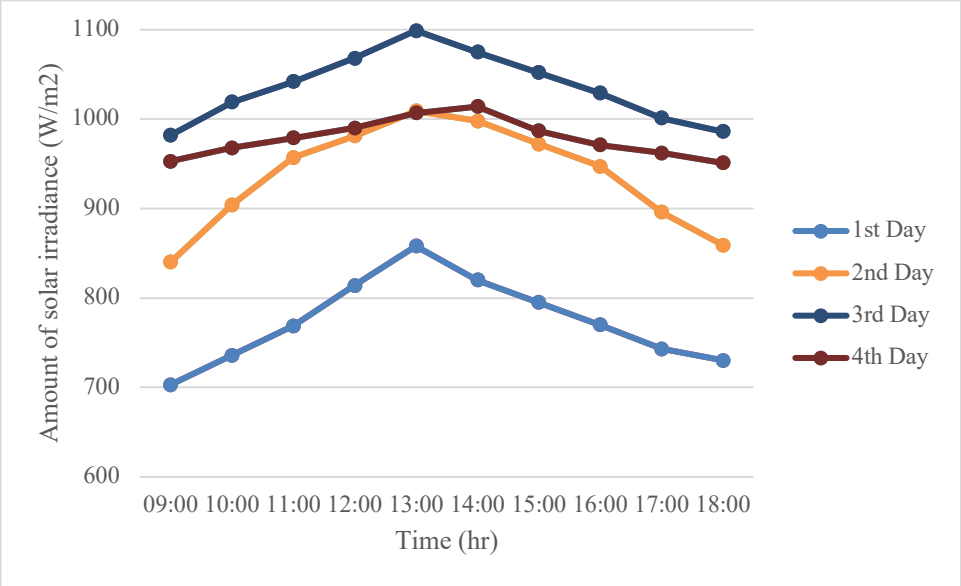

Figure 1. Amount of Solar Irradiance against time for four (4) days

IJESG International Journal of Energy and Smart Grid
Vol 4, Number 1, 2019
ISSN: 2548-0332 e-ISSN 2636-7904
doi: 10.23884/IJESG.

It was observed that the amount of solar irradiance attains it is maximum values between 12:00 to 14:00 for all the testing days and in the third (3rd) day, the solar collector absorbed more solar irradiance. The average solar irradiance harnessed by the collector for the testing days were 773.8W/m^2, 936.3W/m^2, 1035.3W/m^2 and 978.2W/m^2 respectively.

Figure 2 presents the air temperature (ambient, collector, drying chamber and chimney) against time for 24 hours testing when the solar drying chamber was under offloading condition.

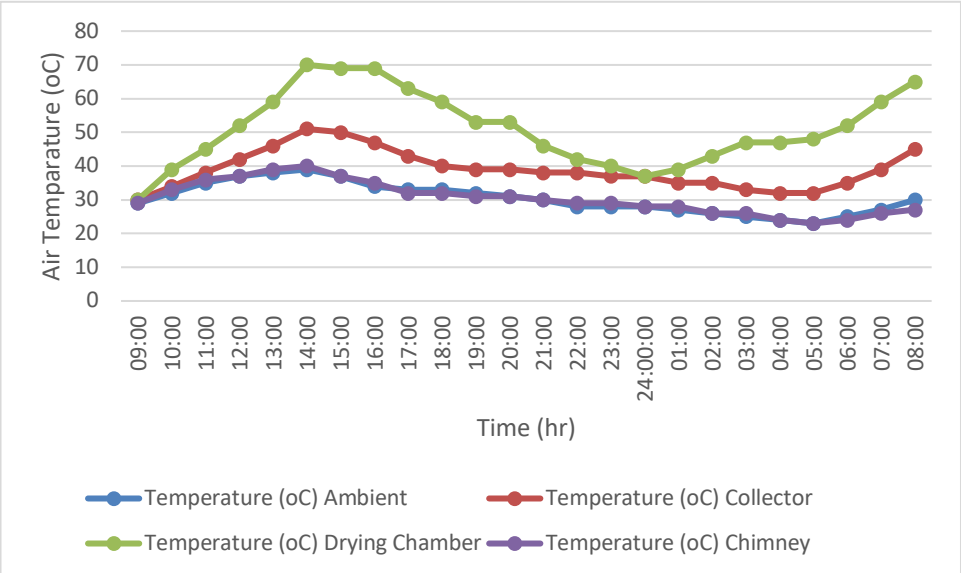

Figure 2. Air Temperature against Time for offloading Condition

From figure 2, the air temperature of all the measuring variables were increasing from 9:00 and reaches their maximum values between 12:00 to 14:00, and then retarded between 15:00 to 20:00. But for drying chamber, the temperature kept increasing between 23:00 to 8:00 this is due to the thermal storage materials that is given out heat stored in the evening or during cloudy hours.

It was also found that the temperature for drying chamber was always higher with an average of 51.08ºC and it has peak value of 70ºC at 14:00 when the ambient temperature was 39ºC, the average ambient temperature was 30.46ºC, which is 20.62ºC less than that of drying chamber, a similar result was reported by [5].

Figure 3 shows the relative humidity with respect to time for offloading condition.

IJESG International Journal of Energy and Smart Grid
Vol 4, Number 1, 2019
ISSN: 2548-0332 e-ISSN 2636-7904
doi: 10.23884/IJESG.

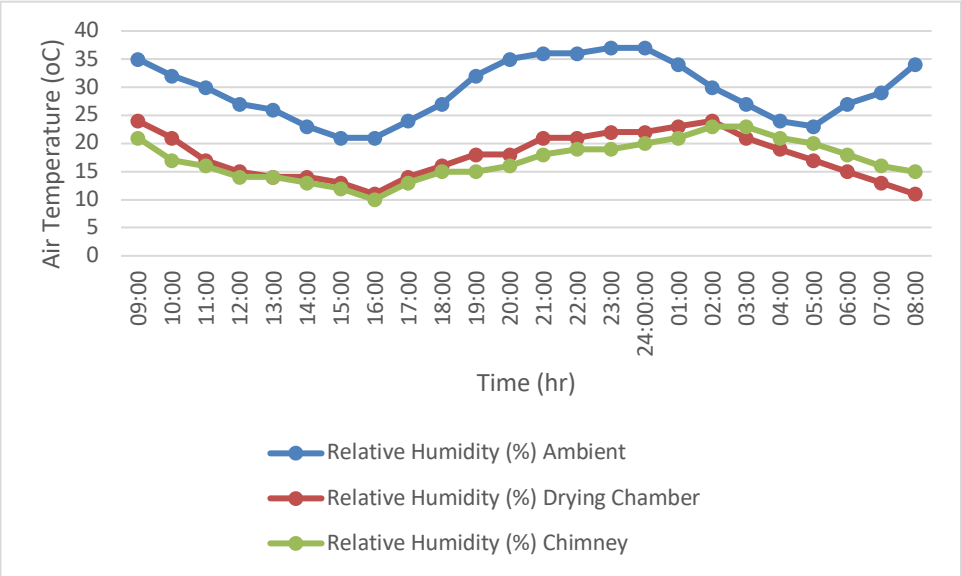

Figure 3. Relative Humidity versus Time for Offloading Condition

It was found that the relative humidity for ambient, drying chamber and chimney outlet were decreasing as the sun rise as shown in figure 3. It was observed that the relative humidity at ambient was higher than at any point of measurements (Drying chamber and chimney outlet) and it was decreased from 35% at 09:00 hour to 21% at 15:00 and 16:00 hours respectively. The average relative humidity at ambient, drying chamber and chimney outlet were recorded as 29.46%, 17.67% and 17.04% respectively.

For loading conditions of the solar drying chamber, the air temperature and relative humidity at all measuring points with respective to time were presented in figure 4 and figure 5 respectively.

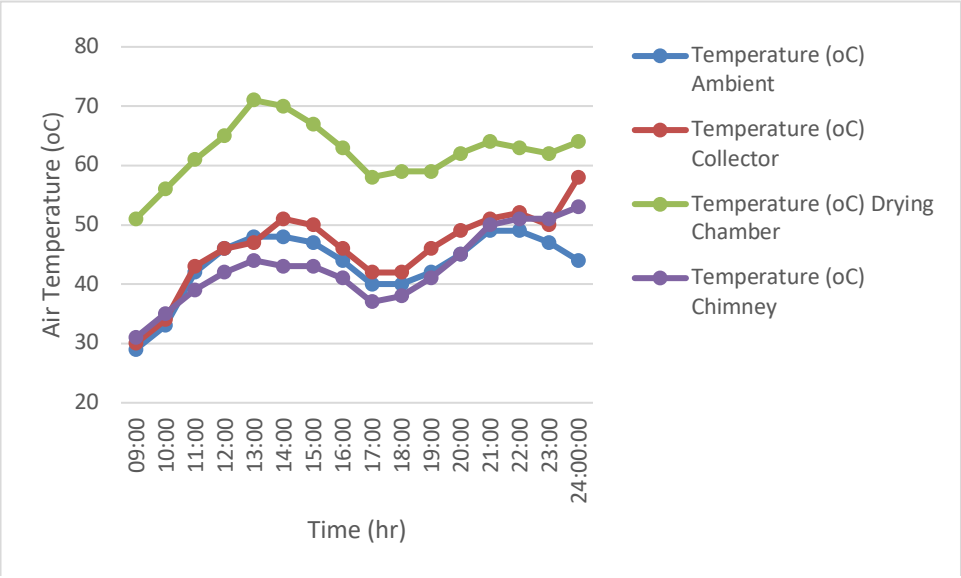

Figure 4. Air Temperature against Time for loading Condition

IJESG International Journal of Energy and Smart Grid
Vol 4, Number 1, 2019
ISSN: 2548-0332 e-ISSN 2636-7904
doi: 10.23884/IJESG.

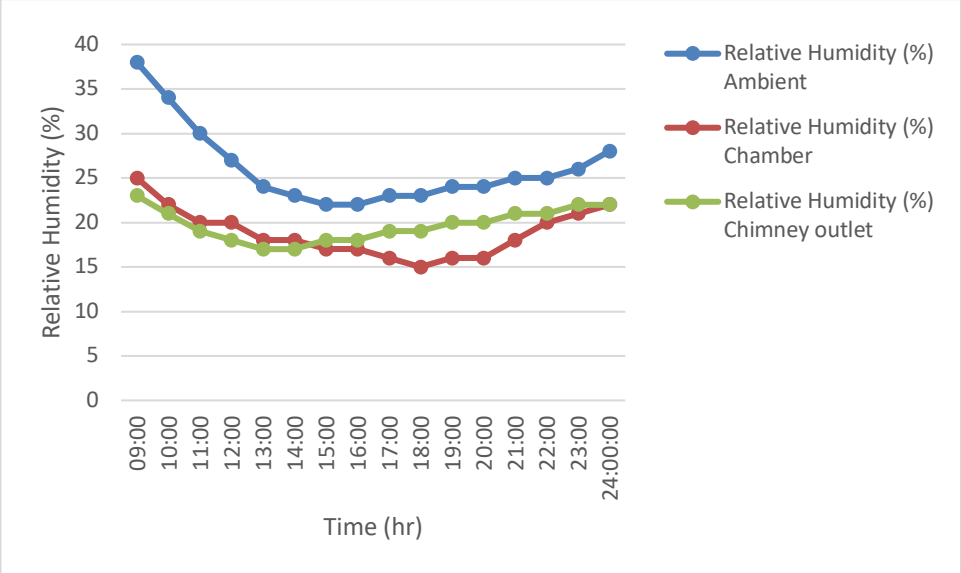

Figure 5. Relative Humidity versus Time for Loading Condition

It was observed that the temperature at drying chamber is higher than that at ambient, collector and chimney, where it attains peak value of 71ºC at 13:00 hour as shown in figure 4, which is closed to the maximum allowable temperature for drying tomatoes (70ºC). The average air temperature at ambient, collector, drying chamber and chimney outlet for loading condition were 43.31ºC, 46.06ºC, 62.19ºC and 42.75ºC respectively. There is significant variation between the air temperatures at drying chamber and ambient, which is 18.88ºC which is within the report of [5].

As shown in figure 5, the relative humidity at drying chamber varied between 15% and 25% at 18:00 hour and 09:00 hour respectively. It was noticed that the relative humidity at all the measuring points were decreasing up to midday and being stable within 13:00 hour to 16:00 hour. This shows that high amount of the moisture from the tomato slices had already been removed, this is supporting the finding of the study conducted by Ezekoye and Enebe [39].

The average wind air at ambient, collector and chimney outlet were 0.32m/s, 0.06m/s and 0.28m/s respectively. The average drying rate of tomato slices was 0.274kg/hr and the quantity of moisture content removed from tomato slices was 58.5% (w.b). The efficiencies of solar dryer and solar collector were found to be 50.2% and 43.03% respectively, for the solar dryer, a similar result was obtained by [40] where they found the efficiency of solar dryer as 56.78%, so also for the efficiency of the solar collector, Struckmann [41] obtained it between 25% to 45%.

5. Conclusion

A hybrid solar dryer was designed and constructed using available materials for drying tomato slices, the performance of the dryer was carried out at Kano, Nigeria with latitude of 12.2º from March

IJESG International Journal of Energy and Smart Grid
Vol 4, Number 1, 2019
ISSN: 2548-0332 e-ISSN 2636-7904
doi: 10.23884/IJESG.

9^{th} to 12^{nd} 2020. The performance of the solar dryer was conducted under two conditions namely: offloading condition and loading condition.

The temperature of hot air measured at the solar collector outlet is always higher than the ambient temperature throughout the testing days for both condition and the temperature inside solar chamber was greater than that at both the ambient temperature and collector, this yield a suitable condition for drying. The drying rate, efficiency of solar collector and drying efficiency were obtained 0.274kg/hr, 43.03% and 50.2%, respectively.

It was found that the solar dryer can dry high initial moisture content agricultural products to the recommended value of moisture content for safe storage within two to three days. The presence of thermal storage material (gravel), therefore, this hybrid solar dryer can be used both day and night/cloudy days.

References

[1] Harringshaw, D., All About Food Drying, The Ohio State University Extension Facts Sheets hygiene, pp. 5347- 5397, 1997. Available at www.ag.ohio-state.edu/

[2] Diamante, L. M., Munro, P. A., Mathematical Modelling of Thin Layer Solar Drying of Sweet Potatos, *Solar Energy,* 51, (2004), pp. 176 – 271

[3] Whitefield, D. E., Solar Dryer Systems and Internet, Important Resources to Improve Food Preparation, *Proceedings,* 2000 International Conference on Solar Cooking, Kimberly, South Africa, 2000

[4] Garg, H. P., Prakash, J., Solar energy fundamentals and applications, *Tata McGraw Hill,* New Delhi, India, 1997

[5] Bolaji, B.O., Performance Evaluation of a Simple Solar Dryer, *6^{th} Annual Engineering Conference Proceedings*, Federal University of Technology Minna, 2005 pp. 8-13

[6] Togrul, I. T., Pehlivan, D., Modelling of Thin Layer Drying Kinetics of some Fruits Under Open Air Sun Drying Process, *Journal of Food Engineering*. 65, (2004), pp. 413- 425

[7] Bassey, M. W., Development and Use of Solar Drying Technologies. *Nigerian Journal of Solar Energy*. 89 (1989), pp. 133- 164

[8] Bukola, O. B., Ayoola, P. O., Performance Evaluation of a Mixed-mode Solar Dryer. Technical Report, *AU J.T*, 11 (2008), 4, pp. 225-231

[9] Akinola, O. A., Akinyemi, A. A., Bolaji, B. O., Evaluation of traditional and solar fish drying systems towards enhancing fish storage and preservation in Nigeria, *J. Fish. Int. Pakistan,*1 (2006), 3, pp. 44-49

[10] Akinola, A. O., Fapetu, O. P., Exergetic Analysis of a Mixed-Mode Solar Dryer, *J. Eng. Appl. Sci.,*1 (2006), pp. 205-210

IJESG International Journal of Energy and Smart Grid
Vol 4, Number 1, 2019
ISSN: 2548-0332 e-ISSN 2636-7904
doi: 10.23884/IJESG.

[11] Akinola, A. O., Development and Performance Evaluation of a Mixed-Mode Solar Food Dryer, M. Eng. Thesis, Federal University of Technology, Akure, Nigeria. 1999

[12] Simpson, W. T., Tehernitz, J. L., Design and Performance of a Solar Lumber for Tropical Latitudes, *Proceeding* on Wood Drying Party, IUFO Division "V" Conference, Oxford, UK, 1980, pp. 59-70

[13] Poonia, S., Singh, A. K., Santra, P., Jain, D., Performance evaluation and cost economics of a low-cost solar dryer for ber (Zizyphus mauritiana) fruit, *Agricultural Engineering Today,* 41 (2017), 1, pp. 25–30

[14] Mustayen, A. G. M. B., Mekhilef, S., Saidur, R., Performance study of different solar dryers: A review, *Renew. Sustain. Energy Review*, 34 (2014), pp. 463–470

[15] Sharma, A., Chen, C. R., Vu Lan, N., Solar-energy drying systems: A review, *Renewable and Sustainable Energy Reviews,* 13 (2009), pp. 1185–1210

[16] Purohit, P., Kumar, A., Kandpal, T. C., Solar drying vs. open sun drying: A framework for financial evaluation, *Solar Energy,* 80 (2006), pp. 1568–1579

[17] Hossain, M. A., Woods, J. L., Bala, B. K., Optimisation of solar tunnel drier for drying of chilli without color loss, *Renewable Energy,* 30 (2005), pp. 729–742

[18] Pangavhane, D. R., Design, Development and performance testing of a new natural convection solar dryer, *Energy*, 27 (2003), 6, pp. 579-590

[19] Ekechukwu, O. V., Norton, B., Review of solar energy drying systems II: An overview of solar drying technology, *Energy Conversion and Management,* 40 (1999), pp. 615–655

[20] Sodha, M. S., Chandra, R., Solar drying systems and their testing procedures: A review, *Energy Conversion and Management,* 35 (1994), pp. 219–267

[21] Kumar, M., Sansaniwal, S. K., Khatak, P., Progress in solar dryers for drying various commodities, *Renewable and Sustainable Energy Review,* 55 (2016), pp. 346–360

[22] Visavale, G. L., *Solar Drying: Fundamentals, Applications and Innovations,* TPR Group, Singapore, 2012

[23] Ahmed, A. G., Design, Construction ad Performance Evaluation of Solar Maize Dryer, *Journal of Agricultural Biotechnology and Sustainable Development,* 2 (2010), 3, pp. 039-046.

[24] Fudholi, A., Sopian, K., Ruslan, M. H., Alghoul, M. A., Sulaiman, M. Y., Review of solar dryers for agricultural and marine products, *Renewable and Sustainable Energy Reviews*, 14 (2010), 1, pp. 1–30

[25] Leon, M. A., Kumar, S., Bhattacharya, S. C., A comprehensive procedure for performance evaluation of solar food dryers, *Renewable & Sustainable Energy Reviews*, 6 (2002), 4, pp. 367–393

[26] Akuffo, F. O., Forson, F. K., Nazha, M. A. A., Rajakaruna, H., Design of mixed-mode natural convection solar crop dryers, *Renewable Energy*, 32 (2007), pp. 2306-2319

[27] Lawrence, D., Folayan, C. O., Pam, G. Y., Design, Construction and Performance Evaluation of a Mixed-Mode Solar Dryer, *The International Journal of Engineering and Science,* 2 (2013), 8, pp. 08-16

[28] Weefer, K. H., Design, Construction and Performance Evaluation of a Solar Drying System for Crops, Master thesis at African University of Science and Technology, Abuja, Nigeria, 2017

[29] Sevik, S., Design, experimental investigation and analysis of a solar drying system, *Energy Conversion and Management,* 68 (2014), pp. 227-234. https://doi.org/10.1016/j.enconman.2013.01.013

[30] Alta, D., Bilgili, E., Ertekin, C., Yaldiz, O., Experimental investigation of three different solar air heaters: Energy and exergy analyses, *Applied Energy*, 87 (2010), pp. 2953-2973. https://doi.org/10.1016/j.apenergy.2010.04.016

[31] Kamble, A. K., Pardeshi, I. L., Singh, P. L., Ade, G. S., Drying of Chilli using Solar Cabinet Dryer Coupled with Gravel Bed Heat Storage System, *Journal of Food research and technology*, 1 (2013), 2, pp. 87-94

[32] Karlekar, B. V., Desmond, R. M., *Engineering heat transfer,* West Publishing Company, U.S.A., 1982

[33] Sreekumar, A., Development of solar air heaters and thermal energy storage system for drying applications in food processing industries, Ph.D Thesis at Cochin University of Science and Technology, Kochi-22, India, 2007

[34] Waziri, N. H., Usman, A. M., Enaburekhan, J. S., Optimum Temperature and Solar Radiation Periods for Kano using Flat Plate Collector, *Journal of Engineering, Design and Technology,* 13 (2015), 4, pp. 570-578

[35] Ceankoplis, C. J., *Transport Process and Unit Operations,* 3rd Edition, Prentice-Hall Internat, Englewood, UK, 1993

[36] Mohanraj, M., Chandrasekar, P., Performance of Forced Convection Solar Drier Integrated with Gravel as Heat Storage material for Chilli Drying, *Journal of Engineering Science and technology,* 4 (2009), 3, pp. 305-314

[37] Drew, F. S., Development and Evaluation of a Natural Convection Solar Dryer for Mango in Rural Haitian Communities, M.Sc. Thesis, University of Florida, USA, 2011

[38] Ezekoye, B. A, Enebe, O. M., Development and Performance Evaluation of Modified Integrated Passive Solar Grain Dryer, *Pacific Journal of Science and Technology*, 7 (2006), 2, pp. 185- 190

[39] Kapadiya, S., Desai M. A., Solar Drying of Natural and Food Products: A Review, *International Journal of Agriculture and Food Science Technology,* 5 (2014), 6, pp. 565-573

IJESG International Journal of Energy and Smart Grid
Vol 4, Number 1, 2019
ISSN: 2548-0332 e-ISSN 2636-7904
doi: 10.23884/IJESG.

[40] Onigbogi, I. O., Sobowale, S. S., Ezekowa, O. S., Design, construction and evaluation of a small-scale solar dryer, *Journal of Engineering and Applied Science,* 4 (2012), pp. 8-21

[41] Struckmann, F., Analysis of a Flat-plate Solar Collector. Report No. 2008 MVK 160, Lund University, Lund, Sweden, 1993

IJESG International Journal of Energy and Smart Grid
Vol 5, Number 1-2, 2020
ISSN: 2548-0332 e-ISSN 2636-7904

INESEG

HARMONIC DISTORTION OF INPUT CURRENT INDUCTION MOTOR ACCORDING TO SWITCHING FREQUENCY IN OFF-GRID PHOTOVOLTAIC SYSTEMS

Suleyman Adak[1] , Hasan Cangi[2]

[1]Mardin Artuklu University, Electrical and Energy Department, Mardin, Turkey, suleymanadak@yahoo.com,
[2]HasCan Engineering Company, Mardin, Turkey, hasancangi@yahoo.com

Abstract: *The proposed solar system is a combination of solar array, boost DC/DC chopper, DC/AC inverter and three-phase squirrel cage induction motor. This paper is dealing with the design, modeling and simulation of squirrel cage induction motor input current total harmonic distortion depending on switching frequency. The relationship between switching frequency (f_{sw}) and total harmonic distortion for current (THD_I) is examined in this paper. Hereby, an inverse relationship is observed between the f_{sw} and THD_I. PV system is modeled by using Matlab/Simulink and detail study has been carried out for this study in order to evaluate the performance of photovoltaic (PV) off-grid system. The design, modeling and simulation of this topology have been performed from 250 Hz to 51 kHz at switching frequency. Satisfactory performance was achieved for reduction harmonic distortion especially above 1 KHz switching frequency values. Low harmonic distortion has many benefits in power systems such as noiseless operation, less power loss and long life. Therefore, it is presented the Modeling & Simulation of solar inverter feeds three-phase squirrel cage induction motor in Matlab/Simulink software programming. Analytical expression of relationship between THD_I and switching frequency has been obtained by curve fitting method consequently.*

Key words: *Switching frequency, Solar array, Curve fitting method, Total harmonic distortion for current (THD_I), Stand-alone PV system*

1. Introduction

Solar energy is one the most important of the renewable resources that use the abundant and free energy from the sun having clean, inexhaustible and environment friendly cyclic operations. It is a scientific fact that the energy of the rapidly increasing demand against available energy resources a very short time will run out [1]. Off-grid PV Systems are mainly designed to operate independently of the electrical network. PV panel, which converts sunlight to electrical power. The use of photovoltaic

IJESG International Journal of Energy and Smart Grid
Vol 4, Number 1, 2019
ISSN: 2548-0332 e-ISSN 2636-7904
doi: 10.23884/IJESG.

systems as clean source of energy from the sun has been quickly increasing. PV energy is most popular owing to its major advantages, such as no fuel and no pollution [2, 3]. This paper is regarding the design, modelling and simulation of input current squirrel cage motor harmonics distortion depending on switching frequency.

The relationship between switching frequency and input current of squirrel cage induction motor THD_I are examined in this article [4-6]. Thus, an inverse relationship is observed between switching frequency and input current of squirrel cage induction motor THD_I. The schematic diagram of the system is as shown in Figure 1.

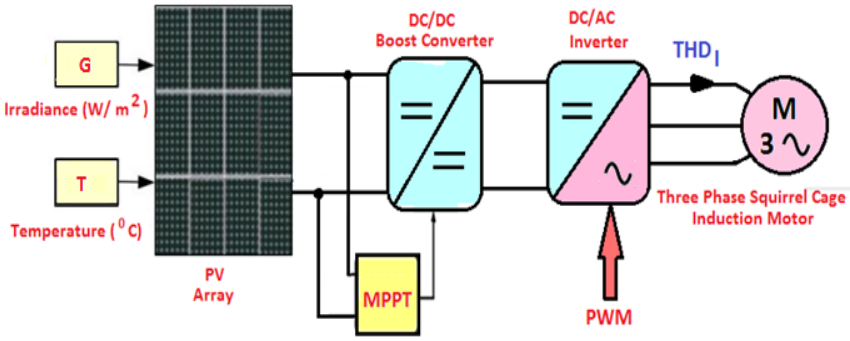

Figure 1. Schematic Representation of Off-Grid System

The cells are designed in modules then modules are interconnected as arrays. The modules might have top out point power depending upon the intended application ranging from few watts, to more than 300 Watts. The ordinary arrays can provide the power by the line-up of 100 Watt-kilowatt, while megawatt arrays do exist. The most important reason for the deterioration of the voltage waveform, the correlation between the terminal voltage and current with non-linear loads are non-sinusoidal sources. Even if nonlinear loads are low powering solar system, they distort sinusoidal current and voltage waveforms. Harmonic components causing serious pollution problem solar system, and they also reduce the quality the energy supplied to the load or consumer. Changing of sun light irradiance also affects the amplitude of the harmonic components. To maximize of output power PV system, repeatedly tracking the maximum power point (MPP) of the system is necessary. The MPP be linked temperature and irradiance of panel and the PV power system simulate by using Matlab/Simulink program [5-7].

2. Harmonics Distortion in Solar Energy System

Harmonic currents generated by non-linear electronic loads, or non-sinusoidal sources. Harmonics increases day by day in solar power system. As a result, harmonic components causing serious pollution problem in solar power system, and they also reduce the quality of energy give to the load. In addition they cause heat losses and resonance problems in solar system. Solar inverters, DC/DC boost converter and battery chargers are the most significant harmonic sources in PV power systems. The input current of the squirrel cage induction motor used in the Simulink circuit is as given in Equation (1).

IJESG International Journal of Energy and Smart Grid
Vol 4, Number 1, 2019
ISSN: 2548-0332 e-ISSN 2636-7904
doi: 10.23884/IJESG.

$$1.341Sin(17\omega t - 98.11) + 1.495Sin(19\omega t - 97.7) \quad (1)$$

The stator current of three phase squirrel cage induction motor is as shown in Figure 2.

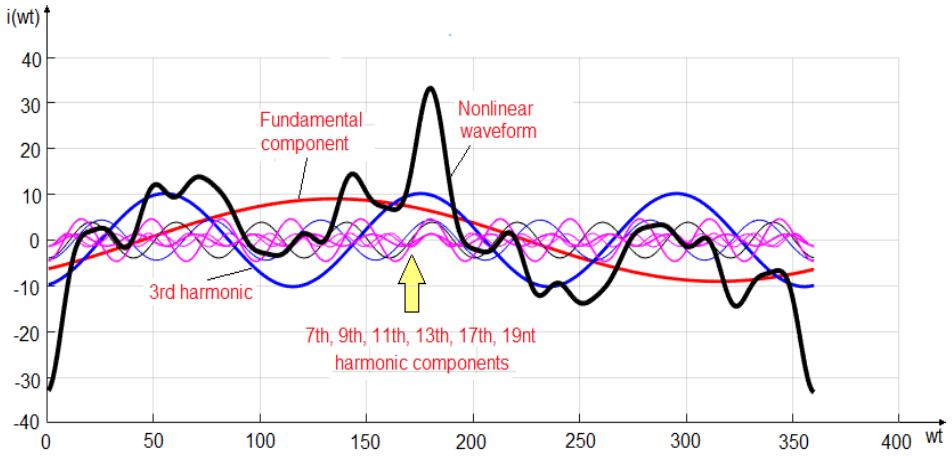

Figure 2. Squirrel cage induction motor stator current and harmonic components (at 250Hz switching frequency)

The converters which used in off-grid PV system are the great harmonic source. Voltage and current harmonics are created by nonlinear loads, and these harmonics cause many problems. The harmonics generated in the PV power converting systems greatly vary with the solar irradiance. The odd harmonics have greater impacts on power quality than even harmonics as they have higher magnitude [8-10]. The current THD is more sensitive on the fluctuation of solar irradiance than the respective voltage THD. Current THD greatly decreases with the increase in the solar irradiance while voltage THD slightly increases with increase in solar irradiance. Power factor varies linearly for values of solar irradiance lower than 200 (W/m^2) and remains close to unity for higher solar irradiance values. In addition, reactive power injection increases at low irradiance. Such as increasing power losses, degrading the conductors, and have negative effect on the distribution systems and other electrical segments [9-11]. Harmonic distortion is generally caused by a nonlinear waveform in PV power systems. Harmonics in the power PV system will cause in the following damage:

- Overheating of solar PV equipment such as solar cables, converters, battery and PV panels
- Incorrect operation of MPPT algorithm.
- Increased internal energy losses in PV power system.
- Causing elements failure owing to high total harmonic distortion.
- Shortened life span of PV device.
- False triggers converters of power electronics.
- Errors measurements voltage, current and power in PV system.
- Increased voltage drop in PV solar system.
- Changes of power factor in the PV system.

THD_I or Total harmonic distortion for current is a common measurement of the level of harmonic distortion present in electrical power networks. The THD_I term expresses as effective value of the all

IJESG International Journal of Energy and Smart Grid
Vol 4, Number 1, 2019
ISSN: 2548-0332 e-ISSN 2636-7904
doi: 10.23884/IJESG.

harmonics, divide by the effective value of its fundamental of current. The distortion as a percentage of total harmonic distortion for current is defined as follow:

$$THD_I = \frac{\sqrt{\sum I_n^2}}{I_1} \quad (2)$$

Where In, is the effective current of the nth harmonics, I1 is the effective current of the fundamental frequency. THD_I or Total harmonic distortion for current is a common measurement of the level of harmonic distortion present in electrical power networks. If the harmonics components are equal to the "0", total harmonic distortion will be equal to the "0" where, In, is the effective voltage of nth harmonic and n=1 is voltage of the fundamental frequency. Voltage and current waveform distortion due to harmonics can lead to the solar system and electrical consumer either damaged or out of order. The analytical solutions and Matlab/Simulink applications have been observed that fit harmonic components occur in the solar power system. The presence of harmonic currents and voltages of the power system means that the degradation of sinusoidal waves. Deteriorated waves called non-sinusoidal waves [12, 13].

A lot of the harmonic problem is caused by the 3rd component. Since the 3rd harmonic is the highest amplitude after the the fundamental component. 3rd, 5th , 7th etc. harmonics component are in the PV system. The harmonics current also flows from neutral and neutral gets overheated. All harmonics decrease the quality of a power PV system and loads connected to it. triples harmonics are significant because the harmonics in each conductor are in Phase. Triples harmonics can therefore be much more damaging. The low order time harmonic effects can be minimized since both stator and rotor are supplied from converters. Voltage drops may occur in PV power system due to harmonics [14-16].

3. Stand-Alone PV System Configuration

The purpose of this study to find optimal input current distortion of three-phase squirrel cage induction motor. A DC to DC boost converters is used when the voltage required by the inverter. Three-phase inverter transfer energy to three-phase squirrel cage induction motor. The purpose of this study is to analyses relationship between switching frequency and input current distortion of squirrel cage induction motor.

To compute the total harmonic distortion (THD) generated by PV system feeding a three-phase squirrel cage motor, and examine the change input current motor THD_I depends on the carrying frequency of PWM. Thus, we can analyses the harmonic that will be generated by the PV systems and thus, design the circuit in Matlab/Simulink. Many techniques were proposed to reduce the size of the direct current (DC) link capacitor while maintaining a good inverter power quality so that a more reliable film type capacitor can be used [15-18]. The smallest unit of PV systems is photovoltaic cell. A PV cell is solid-state semiconductor devices which generates electricity when it is exposed to the light so that PV cell can generates around 2, 5 watts at almost 0.48 volt DC and also the cells have to be connected in series and parallel in order to produce high-efficiency in solar energy applications.

The distortion of input current of squirrel cage induction motor can be reduced by changes of switching frequency. The topologic of off-grid PV system is given in Figure 3, which consists of PV array, a boost DC chopper and three phase inverter connects at three-phase squirrel cage induction

IJESG International Journal of Energy and Smart Grid
Vol 4, Number 1, 2019
ISSN: 2548-0332 e-ISSN 2636-7904
doi: 10.23884/IJESG.

motor. There are two operational modes in the system according to the different working statuses of PV panels, battery and mains supply. The Matlab/Simulink software package can be advantageously used to simulate solar PV system, and analysis of solar inverter. DC link in solar system contains pulsation. Large electrolytic capacitors are connected to the DC link so as to absorb this pulsation so that the DC link voltage ripple can be kept small. The all PV system has been simulated with Matlab/Simulink program. Model off-grid PV system is as shown in Figure 3.

Integrated system has PV array as sources of energy. Therefore, the characteristic of energy storage for a PV system will be explained as well as some specification and standards for a off-grid connected PV system. The simulation of total solar inverter system is given in Fig. 6 Solar cell array and battery is connected with IGBT transistor based three-phase inverter, which further connected to the squirrel cage induction motor. Here ideal switch has been used at DC/DC boost chopper. In practical, there should be a voltage drop across it. As here the ideal switch has been used there is no voltage drop. The purpose of article simulation and analysis of PV based solar single-phase inverter output current distortion depends on switching frequency.

Advantage of PWM Techniques are; while practically no current does not flow when the switch is off, as little as negligible voltage drop on the key switch is turned on. In this way, as well as the lack of power loss, PWM technique very much in line with digital control units. The system changes the on-off switching can provide fit that is so much more comfortable. Also in the embodiment relating to communication techniques and PWM duty cycle of the signals used in communication technology often used. Thus, the desired signals on channels with various adjustments can be obtained. The Simulink model of the solar PV system could be used in the future for extended study with different of a boost DC/DC chopper, DC/AC inverter varied topology [17]. The proposed solar system is a combination of a boost DC/DC chopper, DC/AC solar inverter and three-phase squirrel cage induction motor as shown in Figure 3.

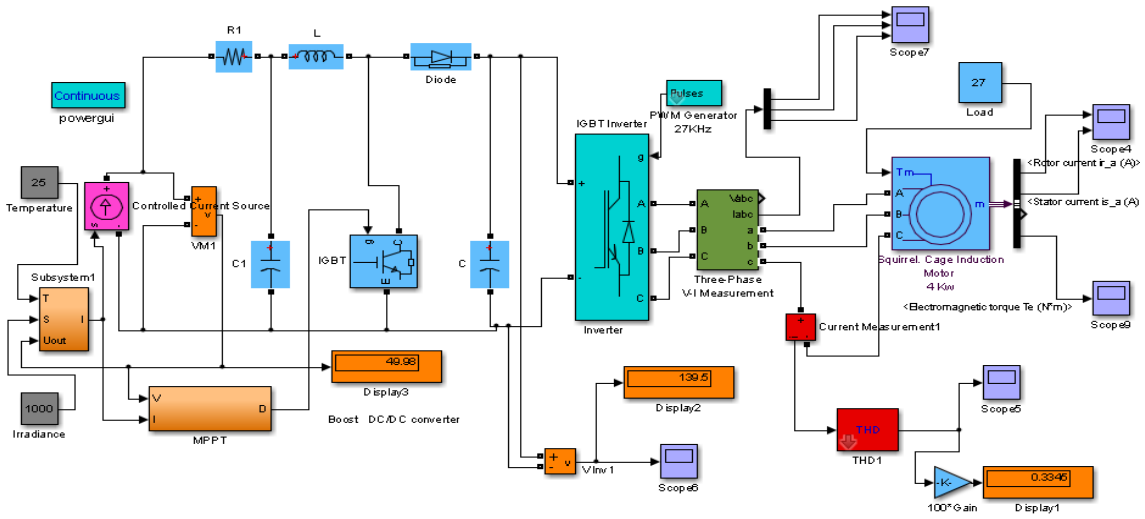

Figure 3. Model Off-grid PV System (27 KHz switching frequency).

IJESG International Journal of Energy and Smart Grid
Vol 4, Number 1, 2019
ISSN: 2548-0332 e-ISSN 2636-7904
doi: 10.23884/IJESG.

The design, modelling and simulation of this topology are performed by using Matlab/Simulink programming for range of 0.6 kHz to 51 kHz of switching frequency. This shows the satisfactory performance of mitigation harmonic distortion at 27 kHz switching frequency. Thus, we present Modelling & Simulation of solar inverter that feeds three-phase squirrel cage motor in Matlab/Simulink software program. The results of relationship between THDI and switching frequency are obtained in Matlab/Simulink software program [19]. Matlab/Simulation has been done for different values switching frequency.

4. Changing of Output Voltage DC-DC Boost Converter

Therefore, the inductor will oppose change or reduction in current. Thus, the polarity will be reversed. There are many types of DC-DC converters such as buck converter, boost converter, and buck-boost converter. Power inverters are electronic device or circuitry that changes direct current to alternating current. Inverter output voltage waveforms not sinusoidal, therefore, they contain harmonics. Output voltage of square wave is acceptable in low and medium power, whereas, in high power applications ask sinusoidal waveforms. Output voltage of a boost DC-DC converter is as shown in Figure 4.

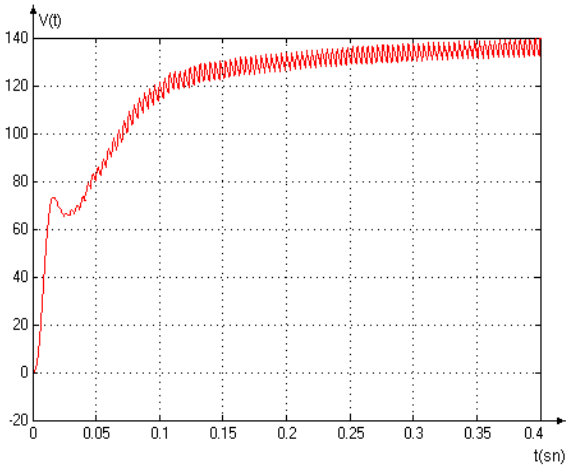

Figure 4. Output voltage of a boost DC-DC converter.

They are connected to the DC bus that could be connected to a different energy storage system, or inject the current directly with a DC/AC inverter. Performance of proposed inverter is verified with exhaustive simulation results on Matlab program. Functions of DC-DC converters have some functions. Capacitor is used to filter ripple currents on DC link. There ripples are caused by power semiconductor IGBT switching. Capacitors are also used to keep the DC voltage stable.

4.1. Electrical characteristics of PV inverter

Inverter which converts the DC waveforms into alternative current (AC) waveforms via a set of solid state switches, here IGBTs are used, that essentially. PV systems use inverters to get connected to

IJESG International Journal of Energy and Smart Grid
Vol 4, Number 1, 2019
ISSN: 2548-0332 e-ISSN 2636-7904
doi: 10.23884/IJESG.

load that utilize alternative voltage. However, solar inverter is a harmonics source. Universal bridge is implemented as IGBT based inverter with parameters as two arm bridge and four pulses. The results of the different switching frequency depend on total harmonic distortion for İNPUT current of squirrel cage induction motor. IGBT based bridges are used as the inverter operating voltage is low and are connected in parallel with each other. This PV inverter convert direct current to alternating current. IGBT is used as switching element in the inverter. PWM generator block is used to produces triggering pulses to IGBT transistor using in single-phase inverter. These pulses are from 0,6 kHz to 51 kHz. The change of inverter output phase to neutral voltage signal is as shown in Figure 5.

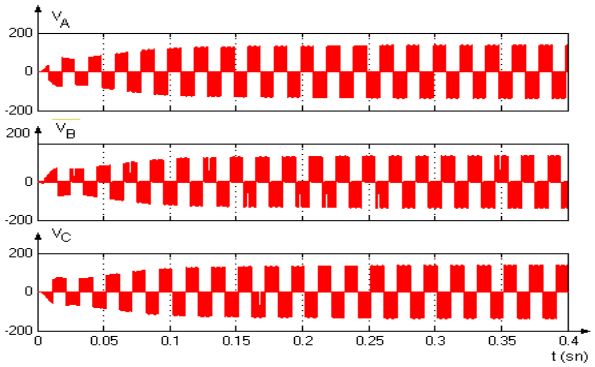

Figure 5. Output voltage of three- phase inverter

The system has been simulated with Matlab/Simulink software program. Solar inverter does not generate excessive noise and harmonics. This study analyzes of input current of squirrel cage motor total harmonic distortion change depending on switching frequency, and also to find the analytic equation between switching frequency (fsw) and THD_I. The simulation is done in Matlab/Simulink software program. Input current of three- phase squirrel cage induction motor is as shown in Figure 6.

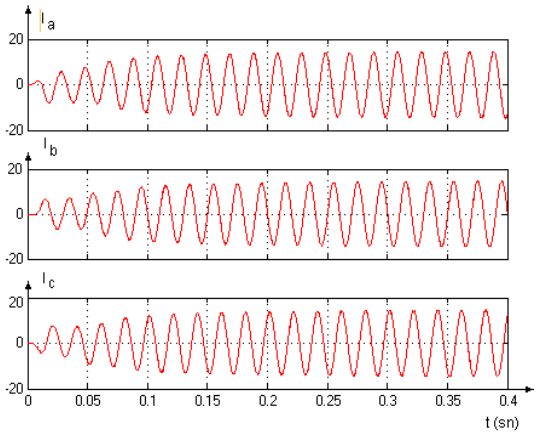

Figure 6. Output current of three- phase inverter.

Solar system structure and working modes are analyzed in detail firstly, then total harmonic distortion belong to switching frequency practical and theoretical analysis based on Matlab/Simulink curve fitting method can be used to summarize the relationships among two or more variables. The

IJESG International Journal of Energy and Smart Grid
Vol 4, Number 1, 2019
ISSN: 2548-0332 e-ISSN 2636-7904
doi: 10.23884/IJESG.

Simulations is carried out as well for validating between switching frequency and THD_I inversely proportional. The change of three- phase squirrel cage induction motor input current THD is as shown in Figure 7.

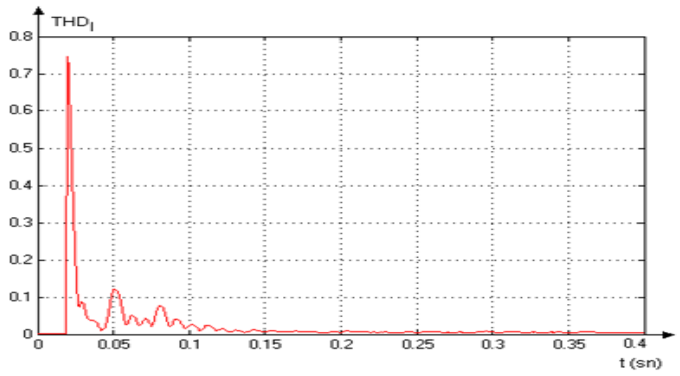

Figure 7. The Change of Squirrel Cage Induction Motor Input Current THD.

The Change of Squirrel Cage Induction Motor Input Current THD becomes stable after 0.4 seconds. No change is observed in THD_I value after 0.4 seconds. Photovoltaic-based inverter outputs current harmonic distortion belongs to switching frequency are primarily discussed in this paper. System structure and working modes are analyzed in detail firstly, and then total harmonic distortion belong to switching frequency practical and theoretical analysis based on Matlab/Simulink. The negative effects of THD_I are such disruption, heating the batteries, overheating the cables, and poor quality of the electrical energy. Total harmonic distortion value was observed that after great value of 1 kHz drop below 5%. At the end of the study, an inverse relationship is observed between the squirrel cage induction motor input current harmonic distortion and the switching frequency.

4.2. Electrical Characteristics of A Three-Phase Squirrel Cage Induction Motor

Induction motors are generally made of two parts, the stator and the rotor. The stator is the standing part of the asynchronous motor. Rotor is the rotating part. The induction motor rotor is of two types, the short rotor (rotor with squirrel cage) and the wound rotor induction motor (rotor with ring). Torque of three- phase squirrel cage induction motor is as shown in Figure 8.

IJESG International Journal of Energy and Smart Grid
Vol 4, Number 1, 2019
ISSN: 2548-0332 e-ISSN 2636-7904
doi: 10.23884/IJESG.

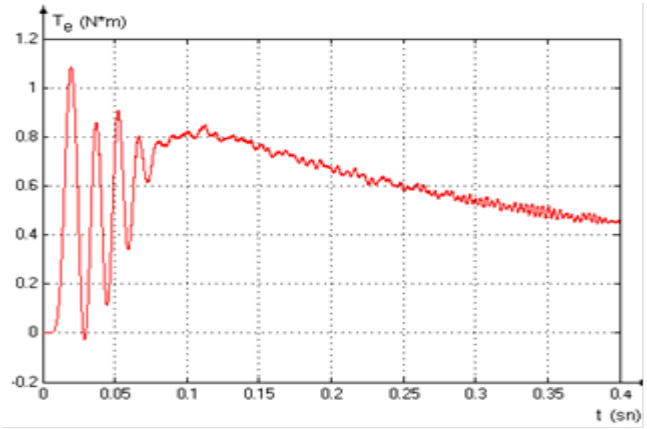

Figure 8. Torque Change Of Three- Phase Squirrel Cage Induction Motor.

The windings, which are placed in the roundabouts in the squirrel cage, are short-circuited with a ring at both ends of the rotor cylinder. In this way, current flows through the shorted rotor conductors to allow rotation of the machine. This engine is also called induction motors with a short-circuit rod. Because induction motors are cheap, do not require too much maintenance and do not make much arc during operation, it is a highly preferred machine.

Even if an asynchronous motor fed from a balanced and pure sinusoidal voltage source, the stator winding distribution due to the internal structure of the machine and therefore the stator ampere-winding distribution is not in sinusoidal form. This cause's structural feature will be released with space harmonics. As a result, currents containing harmonic components will flow through the rotor bars.

Time harmonics will occur if the induction motor is not fed with a voltage in pure sine form. It can be said that the time harmonics are similar effect as space harmonics on the machine. When the harmonic analysis of the source voltage is performed, each component will have effects on the stator and the rotor. Each time the harmonic component will define an equivalent circuit for itself. When the effect of space harmonics is only observed on the rotor, the time harmonics will have an effect on both the stator and the rotor. Rotor and Stator currents of three- phase Squirrel cage induction motor is as shown in Figure 9.

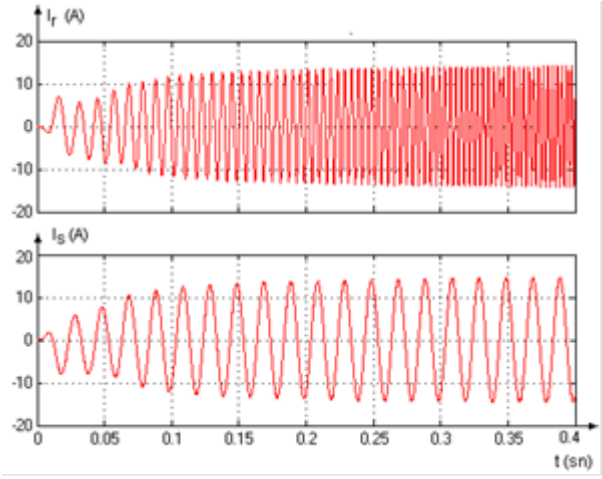

Figure 9. Change of Rotor and Stator Current Squirrel Cage Induction Motor.

IJESG International Journal of Energy and Smart Grid
Vol 4, Number 1, 2019
ISSN: 2548-0332 e-ISSN 2636-7904
doi: 10.23884/IJESG.

Space harmonics must be originated from machine internal structure and they can never be completely filtered. One of the most studied topics in squirrel cage induction motors are the deep groove effect. This will cause an increase in the motor losses.

5. Analytical Equation Between THD_i and Switching Frequency

The main subject of this study is to find the analytical expression of the relationship between switching frequency and the input current squirrel-cage asynchronous motor THD. Curve fitting method was used to find the analytical expression. For different switching frequency, the THD_I values of squirrel cage asynchronous motor are given below, which based on our study.

X=[600, 1000, 1500, 2000, 2500, 3000, 3500, 4000, 4500, 5000, 5500, 6000, 6500, 7000, 7500, 8000, 8500, 9000, 9500, 10000, 10500, 11000, 11500, 12000, 12500, 13000, 14000, 15000, 16000, 17000,19000, 21000, 23000, 25000, 27000, 29000, 31000, 33000, 35000, 36000, 37000, 38000, 39000, 40000, 41000, 43000, 45000, 47000, 48000, 49000, 50000, 51000]

The following THD values are obtained in different values of the switching frequency.

Y=[4.632, 2.729, 1.826, 1.405, 1.153, 0.9716, 0.8552, 0.8403, 0.6894, 0.6416, 0.8755, 0.5748, 0.7452, 0.6369, 0.7478, 0.5945, 0.7931, 0.5999, 0.5146, 0.4588, 0.6032, 0.4144, 0.8663, 0.4544, 0.7052, 0.7087, 0.6271, 1.006, 0.4503, 0.582, 0.7552, 0.5165, 0.4467, 0.4675, 0.3345, 0.5269, 0.6628, 0.5995, 0.4662, 1.277, 0.4394, 0.4466, 2.142, 0.7389, 0.9094, 0.5350, 0.5962, 0.5508, 0.7552, 1.061, 0.5225, 0.6315]

The distortion rate of the inverter output current is completely dependent on the switching frequency. The variation between the switching frequency and the input current harmonic distortion of squirrel-cage asynchronous motor is shown in Figure 10.

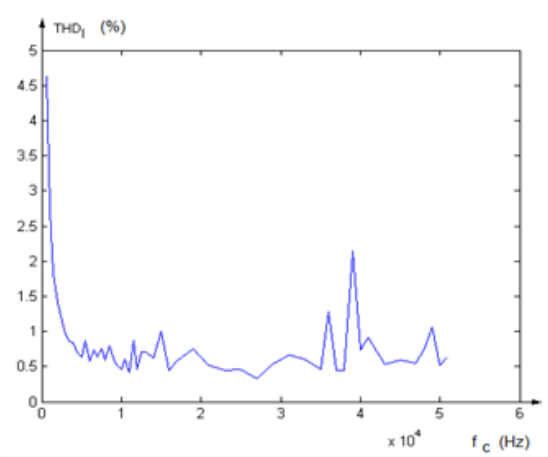

Figure 10. Change of total harmonic distortion depends on switching frequency.

Generally, the data obtained as a result of experimental studies are point values. There is no function definition between the points. So; The “curve fitting” problem is the determination of another

IJESG International Journal of Energy and Smart Grid
Vol 4, Number 1, 2019
ISSN: 2548-0332 e-ISSN 2636-7904
doi: 10.23884/IJESG.

function closest to the function in point-to-point values of a function, or the search for new functions that can facilitate calculations to replace functions that are difficult to use in practice. It is possible to find the equation of the graph in Figure 10 by curve fitting method. To simplify the operations fsw=x, THD_I=y. Assume that the graphic of Figure 10 occurred by the equation as given below;

$$f(x) = k * x^{-m} \tag{3}$$

Let's take both sides logarithm of equation (3),

$$\log\big(f(x)\big) = \log(k) - mlog(x) \tag{4}$$

The equation (6) can be easily represented as follows:

$$\log\big(f(X)\big) = Y, \quad \log(k) = A, \log(X) = X \tag{5}$$

Equation (5) is converted to the linear equation,

$$Y = A + bX \tag{6}$$

To find k and m values,

$$\gg Polyfit(\log(X).\log(Y), 1) \tag{7}$$

As a result,

ans =-0.2533 2.0729

>> a=exp(2.0729)

a =7.9478

values are found. If we put the values of k and m in the equation (3),

$$y = 7.9478x^{-0.2533} \tag{8}$$

equation is obtained. Then, the equation can be written as below;

x=fsw, y =THD_I is put in the (8) equation

$$THD_I = 7.9478 f_{sw}^{-0.2533} \tag{9}$$

(9) equation is obtained . This new (9) equation was obtained at Matlab program by using the curve fitting method. Changing of equation (9) is as shown in Figure 11.

IJESG International Journal of Energy and Smart Grid
Vol 4, Number 1, 2019
ISSN: 2548-0332 e-ISSN 2636-7904
doi: 10.23884/IJESG.

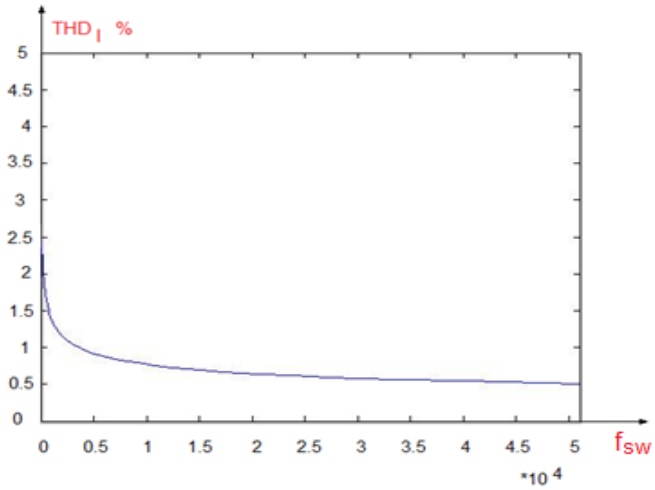

Figure 11. Change of total harmonic distortion depends on switching frequency.

The high THD have negative effects on PV power system such as equipment overheating, motor vibration, neutral overloading and low power factor. As a result of this study, it was observed that there is an inverse proportional change between the switching frequency and the input current of squirrel cage induction motor THD_I.

Table1. Input current distortion of asynchronous motor at different switching frequency values.

fsw (switching frequency	600 (Hz)	1050 (Hz)	9000 (Hz)	27000 (Hz)	40000 (Hz)
THD_I (Total harmonic distortion for current)	1.5733	1.3645	0.7918	0.5995	0.5427

The effect of the switching frequency on inverter output current harmonic distortion is quite high. For less loss and stable operation, harmonic distortion should be kept small for the input current of the squirrel cage induction motor.

6. Conclusion

This study was examined the relationship between switching frequency (f_{sw}) and total harmonic distortion for current (THD_I) by means of using the design, modeling and simulation of squirrel cage induction motor input current total harmonic distortion depending on switching frequency. Harmonic distortion value for the asynchronous motor decreases at high values of PWM's carrying frequency. THD_I of squirrel cage asynchronous motor decreases below 1% when switching frequency is greater than 3 kHZ (f_{sw} > 3 kHZ). Inverse proportional relationship has been observed between f_{sw} and THD_I. The most serious and negative effect of harmonics in rotating machines is overheating especially in rotor and stator circuits. Harmonics cause copper and iron losses in induction machines. The high frequency of harmonic components destroys the rotating magnetic field and causes the machine to work with noise and vibration. In three-phase squirrel cage induction motors, the coil pitch can be shortened to certain values in order to eliminate space harmonics. Analytical expression (Eq.9) was obtained between f_{sw} &

THD_I of the squirrel cage asynchronous motor by using the Matlab software program with the feature of curve fitting method. Satisfactory performance was achieved for reduction harmonic distortion especially above 1 KHz switching frequency values. Hence, harmonic distortions of squirrel cage induction motor values were observed below 5%.

References

[1] Wasfi, M. Solar Energy and Photovoltaic Systems, Multidisciplinary Journals in Science and Technology, Journal of Selected Areas in Renewable and Sustainable Energy (JRSE), February Edition, 2011; 1: 1-8.

[2] Cira, F, Arkan, M, Gümüş, B, Goktas, T. Analysis of stator inter-turn short-circuit fault signatures for inverter-fed permanent magnet synchronous motors. IECON 2016-42nd Annual Conference of the IEEE Industrial Electronics Society; 20-23 October: Published by IEEE, pp. 1453-1457, 2016.

[3] Ren, Y, Zhu, Z Q. Reduction of both harmonic current and torque ripple for dual three-phase permanent-magnet synchronous machine using modified switching-table-based direct torque control, IEEE Trans. Ind. Electron, 2015; 62 (11), 6671–6683.

[4] Errouha, M, Derouich, A, Motahhir, S, Zamzoum, El Ouanjli, O, El Ghzizal, A. Optimization and control of water pumping PV systems using fuzzy logic controller. Elsevier, Energy Report, 2019, 5: 853–865.

[5] Bizon, N, Kurt E, Iana, G. Airflow real-time optimization strategy for fuel cell hybrid power sources with fuel flow based on load following. In: ECRES 2017 5. European Conference on Renewable Energy Systems; 27-30 August : Vizyon Publishing House, pp. 222-230, 2017.

[6] Adak, S, Cangi, H. Analysis and Simulation Total Harmonic Distortion of Output Voltage Three Level Diode Clamped Inverter in Photovoltaic System, Bitlis Eren Üniversitesi Fen Bilimleri Dergisi, 2015; 1: 2147-3129.

[7] Badawy, M O, Yilmaz, A S, Sozer, Y, Husein, I. Parallel Power Processing Topology for Solar PV Applications. IEEE Transactions on Industry Applications, 2014 ; 50(2) : 1245-1255.

[8] Adak, S, Cangi, H. Design of an LLCL type filter for stand-alone PV systems harmonics, Journal of Energy Systems, 2019 ; 3(1) : 36-50.

[9] Verma1, S, Kumar, VH, Khwaja M. Modeling & Analysis of Standalone Photovoltaic System. IJRET: International Journal of Research in Engineering and Technology, 2017; 2(1): 259-265.

[10] Kiliç E, Şit S, Gani A, Şekkeli M, Özçalik H, Riza, H. Neuro-Fuzzy Based Model Reference Adaptive Control for Induction Motor Drive, Turkish Journal of Fuzzy Systems, 2017 ; 8(2) : 63-72.

[11] Mithat U, Mathematical and engineering applications with Matlab. İstanbul, TURKEY: Beta Basım A.Ş, 2004.

IJESG International Journal of Energy and Smart Grid
Vol 4, Number 1, 2019
ISSN: 2548-0332 e-ISSN 2636-7904
doi: 10.23884/IJESG.

[12] Kocatepe, C., Uzunoğlu, M., Yumurtacı, R. Elektrik Tesislerinde Harmonikler, Birsen Yayınevi, İstanbul, 2003.

[13] Cangi H. Düşük Işıma Seviyesinde PV Sistemlerde Harmoniklerin Analizi ve Eliminasyonu. PhD, Kahramanmaraş Sütçü İmam Üniversitesi, Kahramanmaraş, 2019.

[14] Chen BC, Lin, C L. Implementation of maximum power-point-tracker for photovoltaic arrays. in Proceedings of the 6th IEEE Conference on Industrial Electronics and Applications (ICIEA '11) , IEEE, Beijing, China, June pp. 1621–1626, 2011.

[15] İzgi E, Öztopal A, Yerli B, Kaymak MK. , Şahin AD. Short-mid-term solar power prediction by using artificial neural networks. Solar Energy, 2012 ; 86 : 725-733.

[16] Ozdemir A, Erdem, Z. Optimal digital control of a three-phase four-leg voltage source inverter - Turkish Journal of Electrical Engineering & Computer Sciences, 2016 ; 24 : 1310-1322.

[17] Cangi H, Adak S. Analysis of solar inverter THD according to PWM's carrier frequency. IEEE Xplore Digital Library, DOI 10.1109/ICRERA.2015.7418694, INSPEC Accession no: 15807201.2015.

[18] İhsan A.Ç, Özel U. Asenkron motorlarda uzay harmoniklerin yok edilmesi için yeni bir stator oluk tasarımı. AKU J. Sci. Eng, 2018 ;18 : 921-931.

[19] Kong W, Qu R, Huang J, Kang M. Air-gap and yoke flux density optimization for multiphase induction motor based on novel harmonic current injection method. in Proc.22nd Int. Conf. Elect. Mach., Lausanne, Switzerland, Sep. pp. 100–10